RSC Advances

REVIEW

Cite this: *RSC Adv.*, 2023, **13**, 4963

An inclusive review and perspective on Cu-based materials for electrochemical water splitting

Abdul Shakoor Sabir, Erum Pervaiz,* Rafiq Khosa and Umair Sohail

Received 11th December 2022
Accepted 25th January 2023

DOI: 10.1039/d2ra07901a

rsc.li/rsc-advances

In recent years, there has been a resurgence of interest in developing green and renewable alternate energy sources as a solution to the energy and environmental problems produced by conventional fossil fuel use. As a very effective energy transporter, hydrogen (H_2) is a possible candidate for the future energy supply. Hydrogen production by water splitting is a promising new energy option. Strong, efficient, and abundant catalysts are required for increasing the efficiency of the water splitting process. Cu-based materials as an electrocatalyst have shown promising results for application in the Hydrogen Evolution Reaction (HER) and Oxygen Evolution Reaction (OER) in water splitting. In this review, our aim is to cover the latest developments in the synthesis, characterisation, and electrochemical behaviour of Cu-based materials as a HER, and OER electrocatalyst, highlighting the impact that these advances have had on the field. It is intended that this review article will serve as a roadmap for developing novel, cost-effective electrocatalysts for electrochemical water splitting based on nanostructured materials with particular emphasis on Cu-based materials for electrocatalytic water splitting.

1. Introduction & background

The greatest difficulty that the present scientific age has is meeting the enormous demand for energy that the modern era has created. Even while the need for energy around the globe is growing, most of the world's electricity is still generated by the combustion of fossil fuels such as oil, coal, and natural gas.[1,2] The world's population is expected to increase by 26% by the year 2050, bringing the total to approximately 9.7 billion people and pushing the demand for primary energy up by an estimated 50%.[3] Because of the fast-approaching depletion of non-renewable energy sources and the goal to cut pollution, scientists are devoting more time and resources to research clean, renewable energy sources.[4–7] It is possible that in the not-too-distant future, hydrogen will emerge as a significant source of energy since it is non-hazardous and can generate a high energy content using non-depletable, renewable resources such as water and light (photon) energy.[8,9] This potentially renewable fuel is utilized in a wide variety of vehicles, including airplanes, electrical devices, and even spacecraft. It is not possible to extract individual hydrogen molecules because these subatomic particles are an inseparable component of all organic matter, including water and hydrocarbons. Alternative methods include bio-photolysis, dark fermentation, photo-fermentation, integrated fermentation, and artificial photosynthesis.[10–13] Viable choices include hydrocarbon steam reforming, non-catalytic partial oxidation, electrolysis of water, and auto-thermal reforming. Even though there are various other techniques, up to 98% of all hydrogen produced is still derived from fossil fuels. Natural gas makes up 40% of the total, oil makes up 30%, coal makes up 18%, water electrolysis makes up 4%, and biomass can make up as much as 1% of the total.[14–17]

The development of methods for the large-scale production of hydrogen will make it possible to extract hydrogen from substances that already contain hydrogen on their own. The production of hydrogen can be divided into two categories: those that concentrate on the material from which hydrogen is extracted and those that concentrate on the energy source that drives the extraction process.[18,19] In electrolysis of water splitting, most of the dissociation process takes place during the hydrogen evolution reaction (HER) and the oxygen evolution reaction (OER), at the cathode and anode, respectively.[20] The electrochemical water splitting takes input energy of $G = 237.1$ kJ mol^{-1}, which is equivalent to a thermodynamic potential of 1.23 V when performed under ordinary conditions.[21–24] On the other hand, the hydrogen evolution reaction (HER) and the oxygen evolution reaction (OER) have relatively low energy conversion efficiencies because they require significant overpotentials to achieve substantial current densities. This is the reason why these reactions have relatively low energy conversion efficiencies.[25,26] Due to this, potential required for water splitting is higher than 1.23 in the working electrochemical setup.[27]

Despite the many investigations that have been carried out over the past ten years,[28] the noble metal-based catalysts

Heterogeneous Catalysis Lab, Department of Chemical Engineering, School of Chemical and Materials Engineering (SCME), National University of Sciences and Technology (NUST), Islamabad 44000, Pakistan. E-mail: erum.pervaiz@scme.nust.edu.pk

(platinum for acidic water electrolysis and iridium or ruthenium oxides for alkaline water electrolysis) continue to be the most effective. Because they require less overpotential and have better electrocatalytic activity in the real reaction process, they are more practical.[29–32] Their very high prices and little availability make widespread commercial utilization in water electrolysis impossible.[33] Because of the high corrosiveness of the electrolyte, it is also possible for the physical properties of the catalyst to be destroyed; hence, for any application in the real world, these attributes need to be robust and stable[34],[35]. Therefore, it is vital to design catalysts with high activity, low cost, and long-term stability to find a suitable replacement for the catalysts that are based on precious metals.[36–38]

Metal–organic frameworks, often known as MOFs, are a newly discovered family of materials that, despite their great porosity, exhibit exceptional crystallinity and long-range organization.[39] MOFs are constructed from organic ligands and metal ions (or clusters), which serve as the basic elements. MOFs have clusters of metal or ions of metal along with solvent molecules and organic ligands. During MOF-driven catalytic processes, the coordinated solvent molecules, such as water, frequently become unstable. Because of this, the metal centre of the MOF will be coordinatively unsaturated.[40,41] The dynamic structure, design tunability, ultrahigh surface area, and crystalline nature of the material, in addition to its high porosity (90% free volume), contribute to the remarkable optical, electrical, and catalytic properties that come from the material. Their possible applications have lately been researched in a variety of various domains, including carbon dioxide (CO_2) collection, sensing, adsorption, and catalysis.[42–44] MOFs have been the subject of extensive research due to the possibility that they could operate as an active catalyst in the electrochemical and photoelectrochemical (PEC) generation of hydrogen.[43,45–47] Cu-based MOFs offers high stability, electrochemical properties, photochemical properties, high catalytic activity, and stability and due to this, it has been the subject of research for a wide range of applications. Some of these applications include photovoltaics, hydrogen storage, ammonia sensing, absorption, HER, and CO_2 reduction.[48–52]

For the MOF-derived nano porous carbon/Cu electrocatalysts for HER in acid media that were synthesized by Jahan-Bakhsh Raoof *et al.*,[53] a Tafel slope of 34.0 mV per decade was reported at an exchange current density of 1.2 mA cm^{-2}. Sakineh Mandegarzad and her colleagues used a Cu–Pd bimetallic nanoparticle-supported nano porous carbon composite as the electrocatalyst to demonstrate the efficiency of HER in acid conditions. Based on the findings, the overpotential was determined to be 200 mV, and the Tafel slope was determined to be 28.2 V dec^{-1}.[54] Ting Song and colleagues demonstrated that hydrogen evolution might be accelerated by using photocatalysis using visible light in their experiment. The Cu-based MOF demonstrates a variety of desirable characteristics, including a high hydrogen evolution rate (5.7 mmol h^{-1}) and outstanding long-term stability when irradiated with visible light.[55] Meso-Cu-BTC MOF electrocatalyst was prepared with minimal effort using a basic method in alkaline media and had a low overpotential (89.32 mV), onset potential (25 mV), and Tafel slope (33.41 mV dec^{-1}).[52]

In this article, we have provided a comprehensive review of the most recent research on the application of Cu-based materials for electrocatalytic reaction that include the splitting of water molecules. We have also discussed some of the parameters that have the greatest impact on the rate at which water splitting events occur, as well as techniques relating to the synthesis of Cu-based catalysts. The most significant problems that need to be solved in the area of electrocatalytic water splitting are discussed, and some insights gained from recent developments in the production of MOF-based catalysts are presented. It is also stated where future research should go to uncover and rationalise the elements that influence the catalytic performance, with a particular focus on establishing the necessary Cu-based materials functionality and building structure–property links. This is done to achieve the overall goal of discovering and understanding the factors that influence the catalytic performance. The aim is also to present a comprehensive overview of current developments in this rapidly evolving sector, as well as some proposals for the development of highly efficient photocatalysts and electrocatalysts based on copper materials for the purpose of water splitting.

2. Essentials of water splitting

Photocatalysis and electrocatalysis are two methods that can be used to split water molecules.[56,57] These methodologies have the potential to produce hydrogen in the most effective and environmentally friendly manner. It takes a large amount of time to create an O–O bond, which results in the loss of four electrons and four protons, making it a significant bottleneck in the process of splitting water.[58] Electron–hole pairs (e/h^+) are produced in the photocatalyst's conduction and valence bands when the electrical configuration of the photocatalyst is stimulated by light to transition from the ground state to an excited state.[59]

2.1. Photocatalytic water splitting

As demonstrated in Fig. 1a, water can be broken down into its parts, hydrogen, and oxygen, by utilizing photocatalysts. The process of photocatalysis on semiconductor particles can be broken down into three primary stages: (i) the photon absorption having high energy comparted to the semiconductor bandgap, which leads to the hole pair and electron generation in the semiconductor particles; (ii) separation of charges, and shifting of photogenerated carriers in the particles; and (iii) the chemical reaction occurs at the surface between semiconductor particles and photogenerated carriers (for example, H_2O).[60,61] To generate O_2, the energy at the top of the valence band needs to be higher than the oxidation potential of water and to make H_2 and the energy at the bottom of the conduction band needs to be lower than the reduction potential of water.[62] Criteria for photocatalysts are: (i) have a larger charge separation, (ii) have faster charge transportation, and (iii) have a narrow energy gap between their bandgap and band edge.[63]

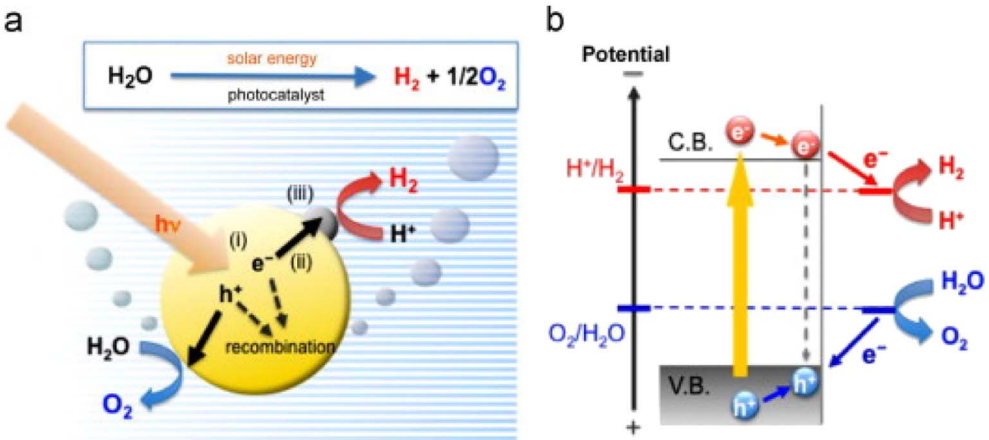

Fig. 1 (a) Illustration of photocatalysis process over semiconductors (reproduced with permission from Elsevier, copyright 2014). (b) Mechanism of electron transfer from valence band to conduction band.[64]

To make the process of H_2 evolution easier, thin layers of semiconductor materials that can be employed for photocatalysis and electrocatalysis is prepared. Different catalysts has been produced for photocatalysis of water splitting *i.e.*, FTO, when analyzing water splitting in the visible spectrum, mesoporous titania thin films produced on fluorine-doped tin oxide (FTO) electrodes were used.[65–68] However, other typical semiconductors such as silicon carbide (SiC), zinc oxide (ZnO), and cadmium sulfides (CdS) are inactive for the process of water splitting. This is because the band gaps of these materials do not align well with the redox potential required for this process, which results in photo deterioration. In the process of photocorrosion, photogenerated holes take the place of water as the oxidant of the anion in the catalyst. In addition, most semiconductor catalysts require ultraviolet (UV) radiation, even though only around 4% of the energy that the sun provides is UV.[69] Because visible light makes up more than half of all incoming solar energy, researchers are actively looking for photocatalysts that work well in the visible light spectrum. This is because these photocatalysts have the potential to increase the efficiency with which solar power is generated. For the band gap of semiconductor materials to be sensitive to visible light, the value of the band gap must be less than 3 eV.[70] Semiconductor catalysts that are combined with carbon materials or precious metal particles have been found to produce a superior response to visible light.[71] In visible light photocatalytic water splitting, metal sulfides, metal nitrides, and metal-free catalysts are all viable options.[72]

2.2. Electrocatalytic water splitting

The production of hydrogen takes place at the cathode of an electrochemical water split, whereas the production of oxygen takes place at the anode. The theoretical minimum voltage needed to split water is 1.23 V ($G = 237.2$ kJ mol^{-1}), according to the equation.[73,74] However, because of kinetics, additional voltage is required on both the cathode and the anode to initiate the reactions. A significant amount of work has been put into inventing outstanding catalysts to reduce the over-potential for complete water splitting. Even though the HER process works best in acidic solutions, full water splitting with non-noble metal catalysts can typically only be achieved in alkaline electrolytes[75] During the water splitting given below reaction occurs in acidic and basic electrolytic media:[76]

In acidic solution.

Reaction at the cathode is:

$$2H^+ + 2e^- \rightarrow H_2 \quad (1)$$

Reaction at the anode is:

$$H_2O \rightarrow 2H^+ + H_2 + \frac{1}{2}O_2 + 2e^- \quad (2)$$

In neutral solution.

Reaction at the cathode is:

$$2H_2O + 2e^- \rightarrow H_2 + 2OH^- \quad (3)$$

Reaction at the anode is:

$$H_2O \rightarrow 2H^+ + \frac{1}{2}O_2 + 2e^- \quad (4)$$

In alkaline solution.

Reaction at the cathode is:

$$2H_2O + 2e^- \rightarrow H_2 + 2OH^- \quad (5)$$

Reaction at the anode is:

$$+2e^- H_2 + 2OH^- \rightarrow H_2O + \frac{1}{2}O_2 + 2e^- \quad (6)$$

Iridium and ruthenium-based materials for the OER and Pt composites for the HER are the most modern catalysts for splitting water in acidic media.[77] A cell voltage of 1.50 V is required to achieve a current density of 10 mA cm^{-2}.[78] Because of the high price and restricted availability of the necessary

materials, the widespread application is impractical. Therefore, a significant amount of effort has been put into the development and synthesis of low-cost alternatives. Many transition metal oxide catalysts, hydroxides, oxyhydroxide catalysts, and perovskite oxide catalysts have been created that have exceptional catalytic performances.[39,79] These catalysts do not require the use of noble metals. There is reason to be optimistic about the catalytic performances of transition metal alloys, nitrides, sulfides, carbides, phosphides, and selenides in the HER.[80] To improve the catalytic activity of underlying catalysts in the process of water splitting, several different ways have been tried. These include manipulating the particle size, shape, dimensionality, composition, and the insertion of defects,[81] as well as utilizing external excitation from light, magnetism, or electric field. Other methods include adjusting the structure of the interface between the two materials.[82]

2.3. Kinetics of hydrogen evolution reaction and oxygen evolution reaction

The hydrogen evolution reaction (HER) is an electrocatalytic mechanism that has received a lot of attention and research. During electrolysis, a HER reaction take place at the cathode. The cathodic hydrogen evolution reaction (HER; $2H^+ + 2e^- \rightarrow H_2$, in acidic conditions) and the anodic oxygen evolution reaction ($2H_2O \rightarrow 4H^+ + O_2 + 4e^-$) are the two components that make up the electrochemical reaction which splits water into hydrogen and oxygen.[83]

Fig. 2a illustrates the functional mechanism of the HER as a process that involves the transfer of two electrons.[84] The Volmer reaction, which includes the release of hydronium ions onto an electrode and ultimately results in the creation of hydrogen intermediates (H*), is what kicks off the HER in an acidic electrolyte. When it comes to alkaline electrolytes, the water molecule itself acts as the proton donor.[85] The production of molecular hydrogen then occurs *via* two distinct pathways, both of which are dependent on the quantity of H* surface coverage that is present. Rate limiting step will be Tafel slop when there will be large quantity of H* atoms will be present. This is because two neighboring H* can combine to generate H_2 molecules. Due to the ability of attracting proton and electron at the same time in acidic conditions and attracting ability of molecules of water and electrons in alkaline media by H* atoms, the Heyrovsky reaction will predominate if there will be low coverage of H*.[86]

Theoretically, the process of splitting water can begin when the thermodynamic potential reaches 1.23 V. Differences in the adsorption energy of hydrogen at the electrode surface cause the kinetics of HER to behave differently depending on the type

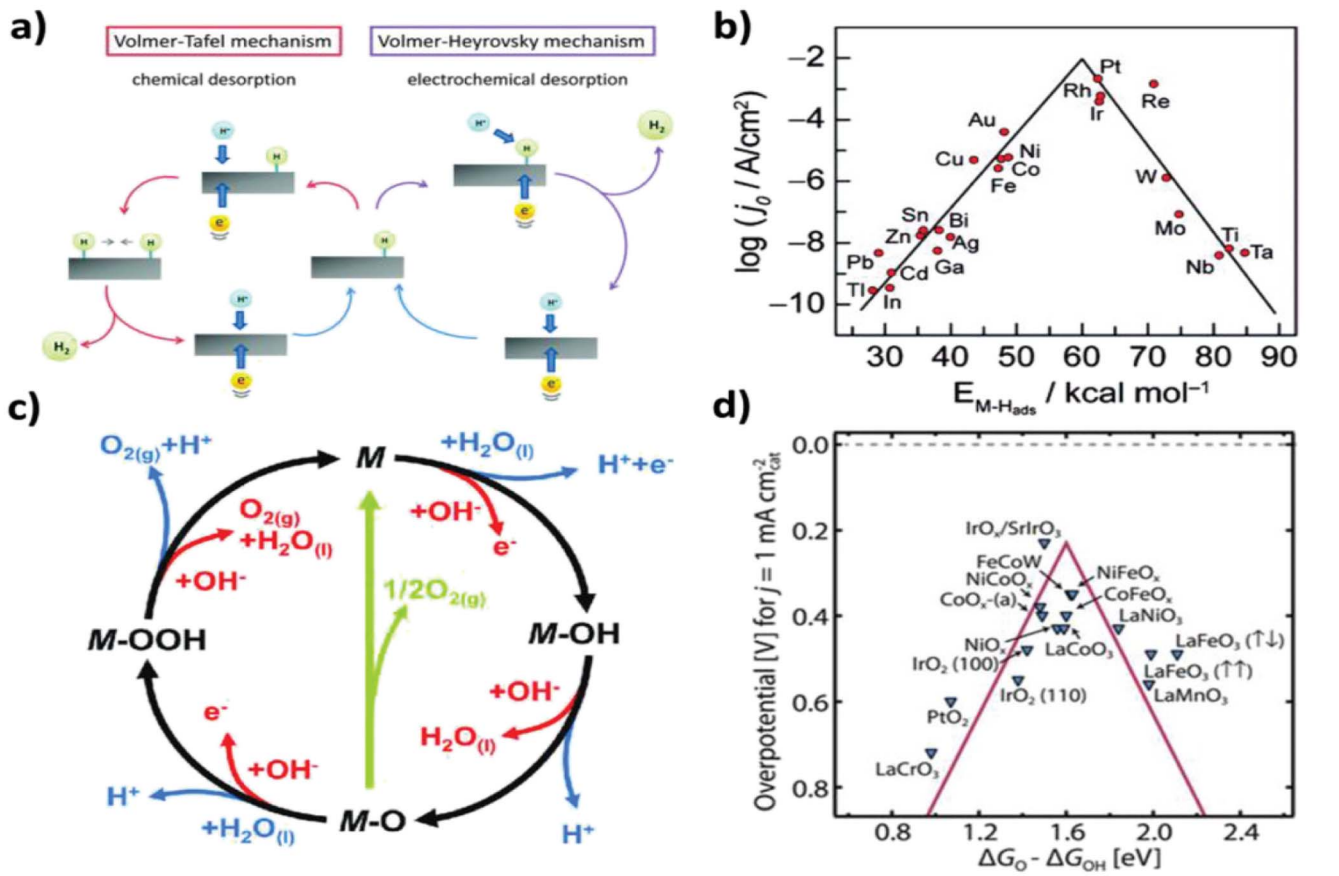

Fig. 2 (a) Two different HER mechanisms of catalysts in acidic electrolytes: Tafel reaction and Heyrovsky reaction. (b) Volcano curve based on metal elements for the acidic HER. (c) Mechanism of OER for both acidic and alkaline media. (d) OER volcano curves based on metal oxides. (Reproduced with permission from *Adv. Mater.*, copyright 2019).[85]

of electrode material used.[87] The applicability of the HER is severely limited due to its poor kinetics and huge overpotential.[88] To enhance the functionality of HERs and raise their level of efficiency, new and superior catalysts need to be created. Electrocatalysts based on noble metals continue to be the most successful kind of HER catalysts, despite the extensive research that has been done into alternative methods. Platinum (Pt), ruthenium (Ru), and iridium (Ir) have a high inherent electrocatalytic activity, and they can be combined with other materials to provide synergistic effects that further boost catalytic performance.[89,90] Platinum (Pt), ruthenium (Ru), and iridium (Ir) have a high inherent electrocatalytic activity. Electrocatalysts that are utilized in the creation of hydrogen require to possess desirable catalytic qualities such as high electrical conductivity, a surface that is highly organized, and a high concentration of electrocatalytically active sites.[91] To be more explicit, the following are requirements that must be met by any electrocatalytic material before it can be utilized in the HER: there is a high level of activity, long-term stability, low level of overpotential, low cost, and scalability potential for mass production.[92]

Platinum (Pt), a particularly uncommon noble metal, is normally the one that is utilized in the role of primary catalyst for HER.[93] Unfortunately, the rarity of precious metals and the high cost of these metals have a negative impact on their commercial value.[94] One of the most important strategies that have been devised is to replace an expensive metal electrocatalyst with an electrocatalyst made of a less expensive material.[95] Nonprecious sulfides, carbides, selenides, phosphides, nitrides, and oxides based on transition metals (such as cobalt, iron, molybdenum, nickel, and tungsten) have garnered a lot of interest because of their promising electrocatalytic activity.[96–101] This is because these nonprecious materials can be used to produce electrocatalysts. Earth-abundant metal electrocatalysts for HER have received considerable attention as a possible solution to these problems since they promise to be highly efficient, affordable, abundant, and long-lasting.[102]

Platinum-group metals (PGM) are widely acknowledged as a benchmark for cathode catalysts across a broad pH range. This is mostly because of the high activity that these metals exhibit toward the HER.[103] The activity pattern of (111), (100), and (001) on the low-index, single-crystal faces of Pt have a significant influence on the HER activity of the metal (110).[104] For this process to take occur, it is necessary to have reactive H_{opd}, which is normally found near the surface. This would imply that the surface of the Pt atom is noticeably more active than those of the other two.[105]

Tang *et al.* synthesized a bifunctional nitrogen-doped graphitic carbon-coated phosphide on carbon cloth (CoP/MoP@NC/CC) with a new structure and a high surface area for general water splitting by using an approach that involved a solid phase.[106] Electrocatalysts were created by applying a current density of 10 mA cm^{-2}, and the resulting electrocatalysts exhibited overpotentials for HER that were lower than those of any phosphide-based composites that had been reported before.[107]

3. MOF as catalysts for water splitting

Metal–organic frameworks, also known as MOFs, are porous crystalline solids with infinite lattices that can be synthesized from secondary building units (SBU), metal cations salts or clusters, and polydentate organic ligands with coordination-type connections.[108,109] These solids are known as metal–organic frameworks (MOFs).[110] MOFs have ultrahigh surface areas that can reach up to 10 000 m^2 g^{-1} when measured using the Brunauer–Emmett–Teller (BET) method. This is much higher than zeolites and active carbons.[111] In the 1990s, research groups led by Moore *et al.*[68], Yaghi *et al.*[108], Kitagawa *et al.*[109] laid the groundwork for MOF constructions and applications.[112] More than 20 000 different MOF structures have been identified, and because of BASF's efforts in mass production, many of these structures are now readily available for purchase *via* a variety of distributors, including Sigma-Aldrich, Strem Chemical, and MOF technologies. MIL-53, HKUST-1, Fe-BTC, and ZIF-8 are among the most widely used MOFs. These materials find use in a variety of industries, including oleochemicals, textiles, transportation, electric vehicle prototypes, food packaging, respiration systems, and chemical sensing.[113]

The conductivity of metal–organic frameworks (MOFs) can be improved by combining them with other nanostructures such as graphene and nanotubes. Graphene and nanotubes are examples of nanostructures that can be combined with MOFs to improve conductivity as can be seen in Fig. 3.

3.1. Synthesis methods of MOF catalyst for water splitting

The methods of synthesis for MOFs are divided into two types which include modern and the conventional method. Sol–gel, electrochemical, and the solvothermal also known as hydrothermal are known as the conventional methods. Although MOFs are synthesized by some modern techniques which includes microwave, sonication, evaporation, and the spray drying.[114] Solvothermal is considered as the most used technique for the synthesis of MOFs. Solvothermal method is carried out based on basic principle of heating reagents which are dissolved in the solvents using autoclave reactor. Then, solvent is used for washing the crystals obtained from the reaction carried out in autoclave reactor. Water and ethanol are most commonly used for washing. In solvothermal technique, organic nature solvents are used *i.e.*, *N*,*N*-dimethyl formaldehyde, and methanol.[115]

Problems associated with solvent process are their hazardous nature and disposal methods. To minimize hazard effects, water is being used as solvent during the washing process for the MOFs synthesis in solvothermal technique. Hydrothermal technique is same as solvothermal with the difference is the use of water as the solvent instead of the organic solvent. The temperature range of solvothermal process is 340–473 K for the heating of the autoclave reactor and the 2–6 days are average processing time. By solvothermal method, well defined crystal structure, crystal size and pore size are obtained high requirement of energy and pressure, and processing in autoclave reactor are bottleneck for solvothermal process.

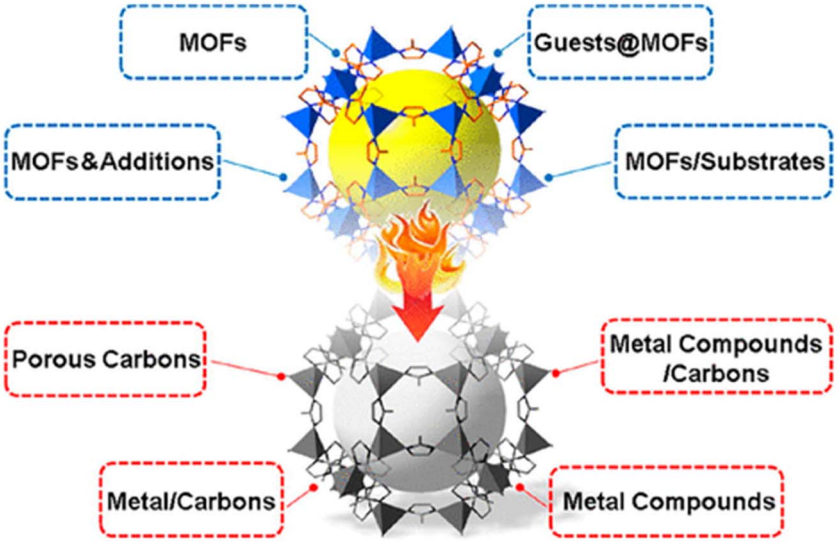

Fig. 3 Classification of MOFs (reproduced with permission from ACS Publications, copyright 2020).[112]

Mechanical method is also being used for the synthesis and obtaining particular configuration of the MOFs crystals.[115] In mechanical method, reagent is stirred for a specified time in the beaker. After stirring, filtration process is used for obtaining MOFs from solvents and then sample is dried in vacuum oven. In mechanical process, the temperature and time required is comparably lower than solvothermal method.

Sono-chemical employ sound frequencies to for the synthesis of MOFs from their respective reagents.[116] In this method, remaining suspensions are filtered out to obtain the fully developed MOFs crystals. Ultrasonication method is most preferred sono-chemical method as it increases the temperature in exponential rate which is necessary for MOFs synthesis and the time required for ultrasonication method is in the range of 1 hour.[117] The salient feature of this method is the high reaction rate and kinetics of the process. The other method of the sono-chemical techniques involves the usage of high frequencies of some audible sound and electricity.[118] These methods are termed as electrochemical method for the synthesis of MOFs. Low pore volume and low surface area are major concerns for ultrasonication method.

Spray drying is a method in which no external forces are employed to bring the desired product.[119] Long period to yield is the biggest drawback of this method.[120,121] Chemical flow method is the other method in which no external forces are used, and, in these techniques, reagents are left in beaker to react completely. The time of synthesis depends upon the completion of the reaction time. The temperature range of spray drying process is 302 K– 573 K. Synthesis by microwave is another method in which reagent are placed in the microwave radiator where reagents reacts under the energy obtained from the radiations.[122,123]

Table 1 provides a comparative study of different methods used for synthesis of MOFs, in which solvothermal method comes out to be the most efficient method as it offers excellent morphology and high crystallinity. According to the literature, solvothermal method is the least energy intensive method comparing electrochemical, microwave, and sono-chemical synthesis methods of MOFs. Solvothermal method also provides high pore volume and surface area comparing other synthesis methods. The major drawback associated with the solvothermal method is its reaction time as it takes 2–6 days to complete the synthesis process comparing other techniques. This compromises the mass production of MOFs on industrial scale.[124] Comparative studies shows that the combination of solvothermal and microwave synthesis process offers high yield and low processing time. The major challenges involved in the MOFs synthesis are: (1) high cost of synthesis. (2) Low yields at industrial scale. (3) Highly energy intensive.

3.2. Applications of MOF catalyst for water splitting

The ubiquitous application of metal–organic frameworks (MOFs) in electrochemical water splitting can be attributed to their high surface areas, adaptable chemical components, configurable pore layouts, and diverse topologies.[127,128] By coupling functional materials such as polyoxometalates (POMs), metal compounds, carbon nanotubes (CNTs), and other conductive substrates as guests @ MOFs or MOF/substrates, it is possible to adapt or modify the characteristics of MOFs.[129] By increasing the number of active sites and the conductivity of the material by a process called functionalization, one can achieve improved electrochemical performance in the process of water splitting.[130]

In a manner comparable to that of other porous materials that perform the function of a catalyst, the metal–organic framework can be utilized in its pure state.[131] When developing pure MOFs for the hydrogen evolution reaction, one must focus their attention largely on the framework configuration as well as the catalytic activity. However, due to its low conductivity and proportional instability in alkaline and acidic environments, it has only been utilized as an electrocatalyst for HER catalysis on a very infrequent basis. To solve the conductivity and instability

Table 1 Cu-MOFs preparation methods and their properties

MOF	Synthesis method and reagents employed	Process	Process conditions	Properties	Merits	Demerits	Ref.
Cu-ABDC	Solvothermal method. Copper nitrate, 2-aminoterephthalic acid, *N N*-dimethylformamide and methanol	All reagents were added in methanol and heated in autoclave. Post heating, the crystals were dried	Stirring the mixture well for 10 min and then constant heating at 110 °C for one day and subsequent vacuum drying at 60 °C	BET SA: 217 $m^2 g^{-1}$ BJT PV: 0.028 cc g^{-1} TGA: thermal limit at 360 °C	Gives good crystallinity and decent BET SA.	Slightly energy intensive	114
Activated carbon-Cu-BTC	Hydrothermal method. Copper nitrate, 1,3,5-tricarboxybenzene, resorcinol, poly (ethylene oxide)-poly (propylene oxide)-poly (ethylene oxide) triblock copolymer, formaldehyde, HCl, ethylenediamine, ethanol and water	All reagents were added in methanol and heated in an autoclave. Post heating, the crystals were dried	Stirring the mixture well at 25 °C for twenty minutes and subsequent heating in an autoclave for a 12 h at 120 °C	BET SA: 1202 $m^2 g^{-1}$ BJT PV: 0.53 cc g^{-1} XRD: bond between metal ion and organic linker unaffected even after the addition of porous carbon. FTIR: presence of carboxyl group. TGA: thermal limit at 600 °C	Presence of fine mesoporous. Very high BET SA. The process has potential for future hybrid sorbents	Process is time taking	125
Cu_3 $(pmtz)_6$ DMF	Solvothermal method. 4,4′,4′′-((1,3,5-triazine-2,4,6-triyl)tris (azanediyl))-tribenzonitrile, NaN_3, NH_4Cl, anhydrous DMF, $Cu(NO_3)_2 \cdot 3H_2O$, acetonitrile, hydrochloric acid	Same as all solvothermal autoclave processes as described above	Stirring the mixture well and subsequent heating in an autoclave for 72 h at 90 °C. After that vacuum drying was done at 120 °C for twenty hours	XRD: Cu–N bonds in the equatorial plane are much shorter than those in the axial direction. TGA: thermal limit at 573			126

Table 2 MOF based catalysts performance summary

Sr. no.	Catalyst hybrid	Medium and study type	Overpotential (10 mA cm^{-2})	References
1	Ni–Fe–Mn-MIL-53	KOH (1 M) OER study	236	141
2	Fe–Ni-MOFs	KOH (1 M) OER study	221	142
3	Cu-MOF with $Fe(OH)_x$	KOH (1 M) HER	112	143
4	MOF/Pt	KOH (1 M) HER	28	144
5	BDC/Co	OER	241	145
6	BDC-Ru–Ni	HER	36	146
7	MOF-74/Fe–Co	OER	280	147
8	Ni-MOF/Co	OER	240	148
9	Ni-MOF/Br	OER	306	149

issue, a great number of methods have been developed to enhance the catalytic activity of untreated MOFs in the hydrogen evolution reaction.[132]

A solvothermal approach was used to produce nitrogen-doped graphene oxide and nickel sulfides (Ni_7S_6). After being chelated with oxygen and nitrogen, the Ni(II) metal centers of the NGO/Ni_7S_6 nano porous composite demonstrated improved catalysis as well as exceptional stability in an alkaline medium for OER and HER. The huge number of pores, high surface area, and availability of nickel at the reaction interface contributed to an increase in the rate of gas release and mass transfer. During the process of optimizing the level of N-doping, the composite's stability was evaluated, and it was shown to be superior to that of the more prevalent RuO_2 and IrO_2 in OER settings. In another study based on graphene composites, ultrathin layers of graphene were used to encase nickel nanoparticles in metal (created from Ni-based MOF using a thermal process in an inert atmosphere). Research has demonstrated that a carbon composite with Co–N doping produced from metal–organic frameworks has a high-performance level and a long lifespan for HER.[133]

During the most recent few years, a great number of materials based on Co-MOF have been developed and implemented on a large scale as electrocatalysts for HER. Liu and colleagues developed Co/NBC by carbonizing cobalt-based boron imidazolate frameworks (BIF-82-Co) at varying pyrolysis temperatures. The resultant Co/NBC-900s in 1.0 M KOH solution was 117 mV, which resulted in a moderate Tafel slope of 146 mV dec^{-1} and a current density of 10 mA cm^{-2} for HER. However, the short stability of these catalysts (10 h) is the primary reason for their restricted applicability.[134]

The performance of MOF composites made by graphene oxide (GO) and carbon nanotubes (CNTs) has been the subject of much investigation, although the results have been inconsistent. The catalytic activity of MOF channels can be improved by placing nanoparticles of sulfides, phosphides, and nitrides in those channels. In this technique of production, MOFs play the role of a scaffold for the nanoparticles, which enables the final dimensions of the nanoparticles to be carefully regulated. The increased immobilization, protection, and selectivity provided by MOFs contribute to the increased stability of NPs. By increasing the conductivity of the MOF, these loaded nanoparticles make HER electrocatalysis more efficient. Pd nanoclusters were immobilized on MOF-67 by Zheng *et al.*, which resulted in the production of a composite material (Pd@MOF-74) with increased electrocatalytic activity.[135] In metal-based MOF composite synthesis,[136] solvothermal deposition was used to functionalize the Zr_6-based metal–organic framework NU-1000 with molybdenum-based MoS_x units. Through the process of thermal decomposition, the platinum nanoparticles and tannic acid coordination polymers were incorporated into a different MOF (ZIF-8).[137,138] Tannic acid shells can be modified by adding metal cations such as nickel, cobalt, copper, manganese, iron, and/or tin. This would result in different chemical compositions. Thermolysis led to the creation of multi-component metal nanoparticles in the metallic fraction of tannic acid, and nanoparticles of platinum served as a seed for this formation. Thermolysis of the organic precursor components was required to create the nitrogen-doped porous carbon capsules with hollow interiors that were determined to constitute the support structure for the nanoparticles. The final catalyst exhibited significantly increased electrocatalytic activity concerning HER.[139] In addition, molybdenum polysulfide (MoS_x) was solvothermal grafted onto Zr-based MOFs (UiO-66-NH_2), which led to an improvement in the performance of the HER (125 mV onset potential at 10 mA cm^{-2} cathode current and 59 mV dec^{-1} Tafel slope at 200 mV overpotential).[140] Researchers found that the results obtained from the 2D Ni-MOF@Pt hybrid produced by incorporating noble metal nanoparticles with modified electronic structure with Ni-based MOF in a highly dispersive way produced better results than those obtained from the individual Ni-based MOF and Pt NPs.[130] This was discovered while the researchers were studying the performance of HER. Table 2 shows the over potential of some MOF hybrids given in the literature.

4. Recent advancements in Cu-based catalysts for water splitting

In contrast to the OER, which makes use of copper-based oxides and hydroxides, HER research is restricted because the copper surface has a low ionic conductivity. This makes it difficult to define the HER kinetics and provide a subsequent energy description when anchoring electroactive species. Graphene and other conducting substrates, innovative methods of

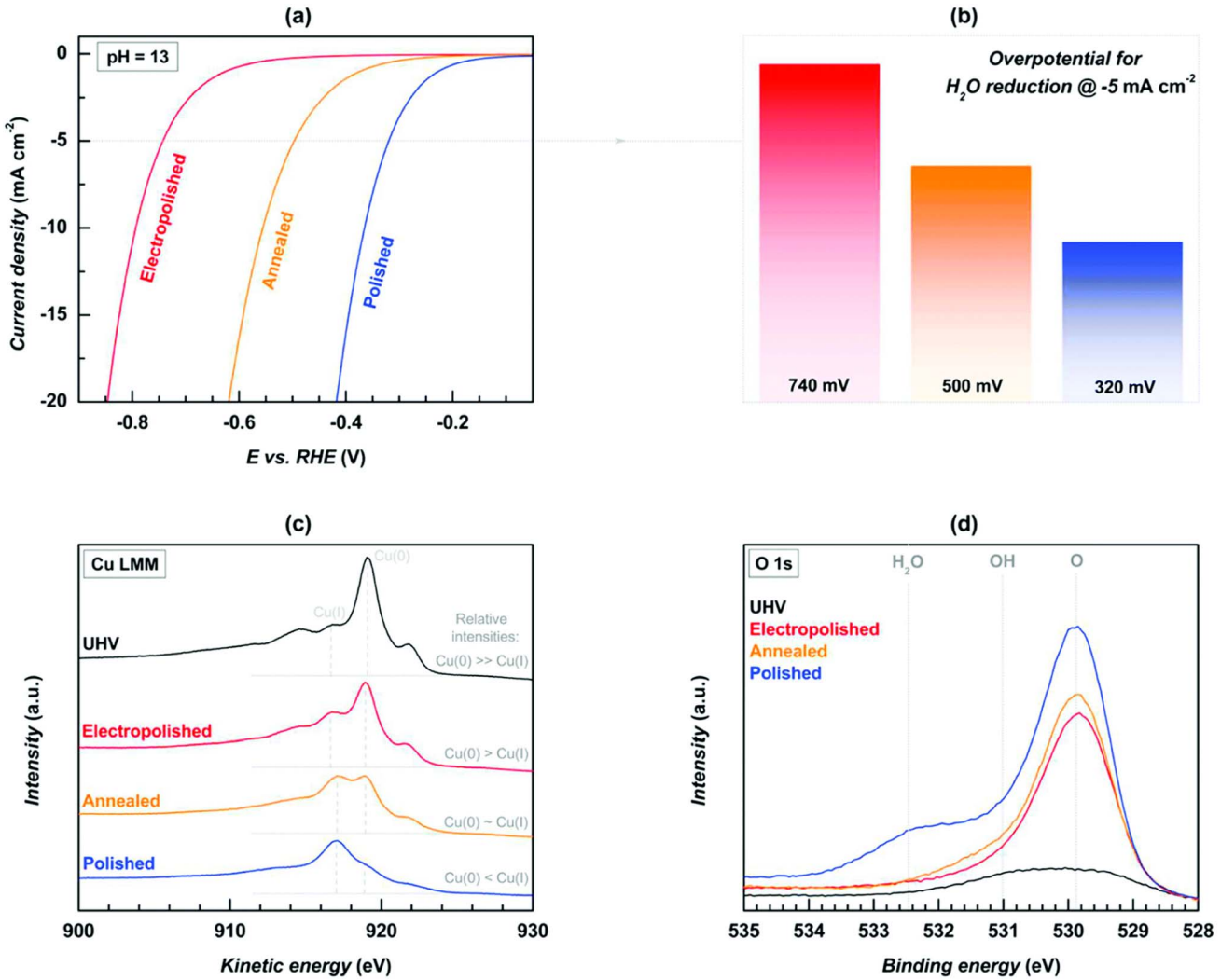

Fig. 4 (a) LSV, (b) value of overpotential at the assigned current density, (c) XPS of Cu-LMM, and (d) spectra of high resolution for O 1a (reproduced with permission from Elsevier, copyright 2019).[151]

synthesis, and the incorporation of other transition metal oxides are some of the potential solutions that have been investigated for the purpose of lowering HER overpotentials and overcoming this resistance in Cu-based oxides. An important study by Farinazzo *et al.*[151] evaluated the effect that electropolishing (E-Cu (poly)), annealing (A-Cu (poly)), and polishing with alumina (P-Cu (poly)) on the surface of polycrystalline Cu in relation to HER under alkaline conditions. When looking at the electrocatalytic activity of HER in alkaline environments, the following pattern was discovered: the following polymers are ranked from excellent to worst: P-Cu (metal) is superior to E-Cu (poly) and A-Cu (poly) (poly). In the XPS investigation, readings that were indicative of the Cu(I) oxidation state (917 eV for the Auger Cu LMM) and the Cu(0) oxidation state (919 eV) were discovered. Researcher were able to characterize the surface chemistry of these electrodes so that they could be used in HER research by analyzing the relative intensities that were measured. At high concentrations, Cu(0) is more dominant than Cu(I), whilst Cu(I) is less dominant, in all three types of E-Cu (poly), A-Cu (poly), and P-Cu (poly) catalysts. Cu(I) is less dominant at lower concentrations. This suggests that the increased HER activity in P-Cu (poly) was ensured by the presence of excess Cu(I). Additionally, this suggests that the overpotential required at 5 mA cm^{-2} is nearly 320 mV, whereas in A-Cu (poly) and E-Cu (poly), the observed overpotentials were 500 mV and 740 mV, respectively. The O 1s XPS high resolution spectra were used to study hydrophilic characteristics, and the results showed that the surface became more hydrophilic after polishing with P-Cu (poly), in comparison to the less active E-Cu (poly) (poly). This study adds to the expanding amount of data that rough Cu-based catalysts can increase HER's hydrophilic properties by pulling in additional electroactive molecules.[150] The body of evidence is growing because of this discovery (Fig. 4).

Copper oxides were coupled with reduced graphene oxide, a metal–organic framework (MOF) porous network, and three-dimensional copper foam by Ye *et al.* to boost the HER activities of the copper oxides. This work is quite intriguing.[152] After

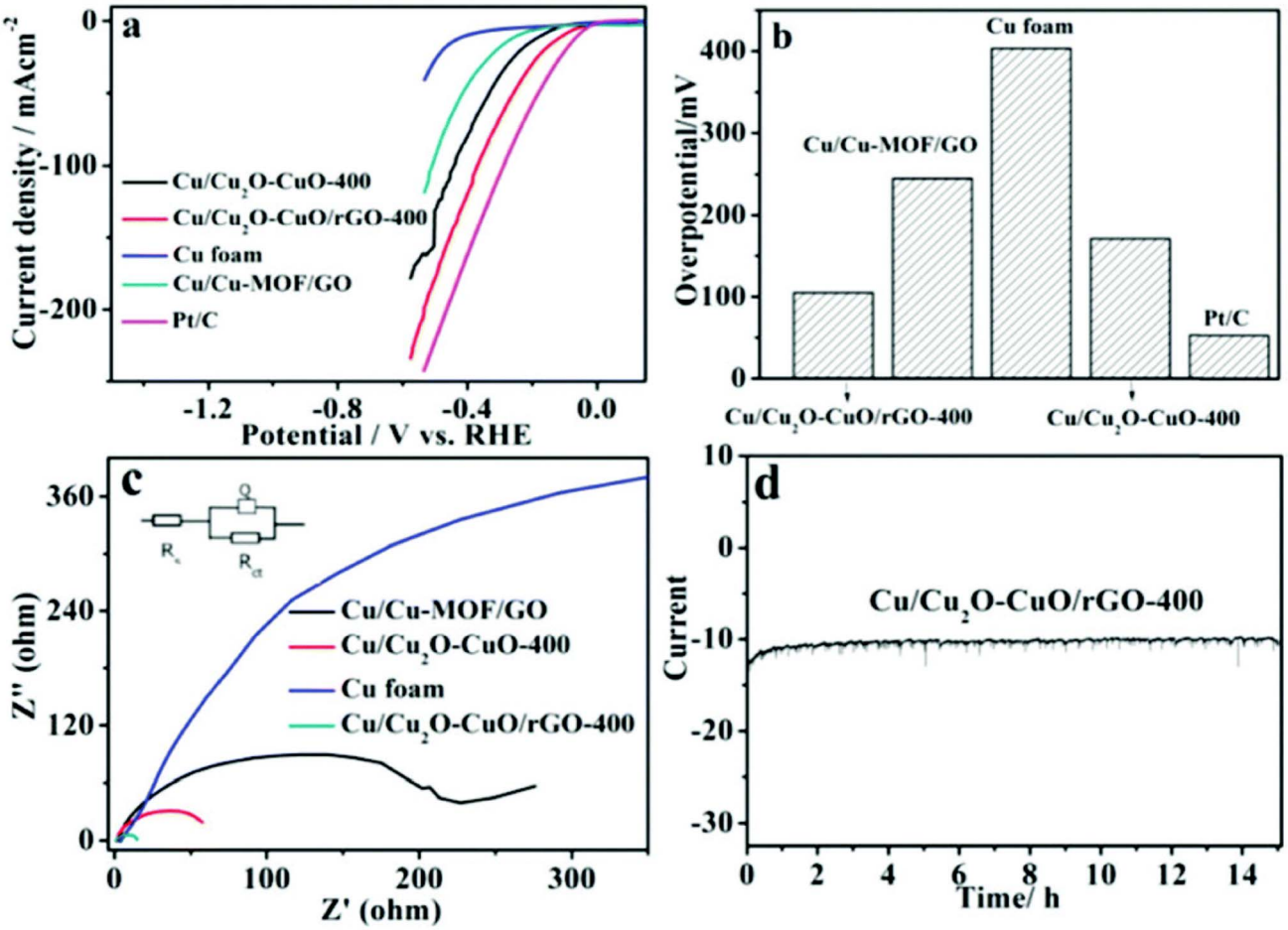

Fig. 5 (a) LSV, (b) value of overpotential at the assigned current density, (c) electrochemical impedance study, and (d) chromatography results obtained for 14 hours trails (reproduced with permission from RSC, copyright 2018).[152]

developing a MOF network on top of the Cu foam, the next step was to add GO in between the two layers to complete the sandwich, which consisted of Cu, Cu, MOF, and GO. It was discovered that Cu/Cu_2O–CuO/rGO, which was created after additional annealing, is an effective HER catalyst when subjected to basic conditions. Cu/Cu_2O–CuO/rGO may demonstrate amazing HER activity, with an onset overpotential of only 84 mV and an overpotential of 105 mV at a current density of 10 mA cm^{-2}, as one would anticipate from electrodes with highly conducting supports and a 3D porous structure. As demonstrated in Fig. 5a, the Cu/Cu_2O–CuO/rGO catalyst showed greater HER activity in comparison to the Cu foam, Cu/MOF/GO, and Cu/Cu_2O–CuO catalysts. This was accomplished by requiring lower overpotentials and attaining higher current densities than the other catalysts. In a similar vein, Fig. 5b suggests that conducting supports such as rGO might improve the kinetics of HER. Further evidence of the superiority of the Cu/Cu_2O–CuO/rGO catalyst in HER can be seen in the fact that it has the lowest R_{ct} among all the catalysts that were tested (Fig. 5c). The catalyst's reliability was validated by a rock-solid consistency, which was observed during a chronoamperometry test that lasted for 14 hours (Fig. 5d). This was in part due to the 3D rGO network's outstanding electrical conductivity, which ensured rapid charge transfer alongside robust activity and structural integrity. This was one of the reasons why this was the case. The findings of this study clear the path for the development of copper-based oxides on metal–organic frameworks (MOFs) and other conductive substrates. This will allow for increased HER activity and stability in basic conditions.

Nanocomposites have the potential to increase HER activity when applied to alkaline media. Tahira *et al.*[153] utilized the dip-coating process to synthesize Co_3O_4–CuO nanocomposites, which demonstrated promising activity in HER. Low HER activity was demonstrated by both Co_3O_4 and CuO; however, the Co_3O_4–CuO nanocomposites required only 288 mV to reach 10 mA cm^{-2} in current density (Fig. 6a). They concluded that the increased activity was brought on by the synergistic boost brought about by the combination of cobalt and copper. The Tafel slope measurements show that the charge transfer kinetics of Co_3O_4–CuO nanocomposites (65 mV dec^{-1}) follow a pattern that is comparable to those of Co_3O_4–CuO and CuO (94 and 243 mV dec^{-1}, respectively) (Fig. 6b). In addition, the composites showed enhanced stability throughout both the potentiodynamic and the galvanostatic trials. These copper oxides for HER research have showed promise for the creation

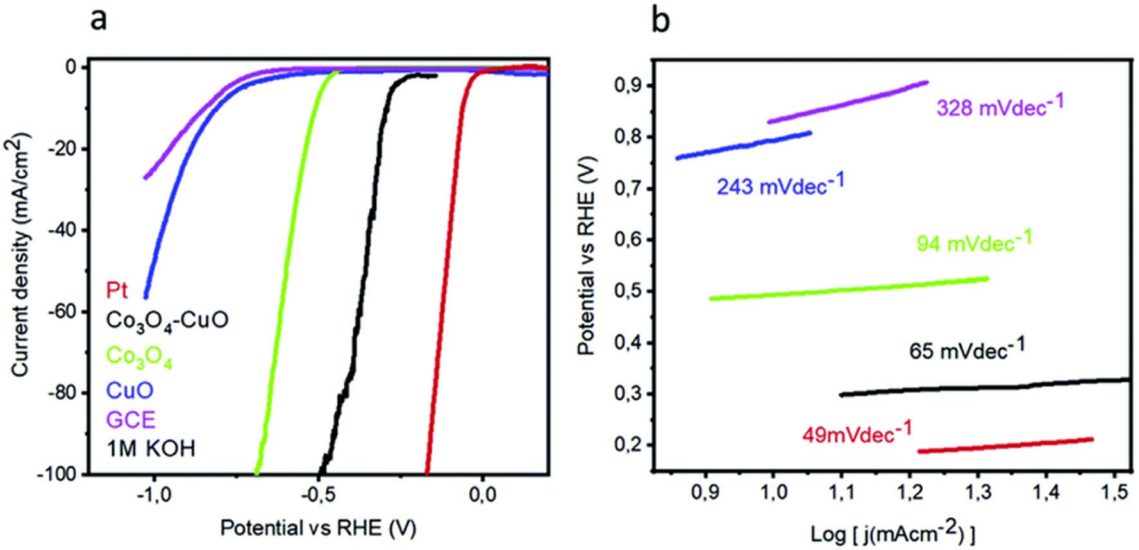

Fig. 6 (a) LSV and (b) Co_3O_4, CuO, and Co_3O_4–CuO nano-based composites taffel slops (reproduced with permission from Elsevier, copyright 2019).[153]

of future catalysts by drawing attention to the necessity of certain modifications that would lead to a greatly higher level of HER activity. Incorporating conducting supports, embedding in three-dimensional foam, utilizing nanocomposites, and other alternative approaches are all being studied as potential ways to improve the performance of Cu-based oxides in HER.

4.1. Cu-based layered double hydroxides for OER and HER

Because of the sequentially layered arrangement of metal sharing octahedrons (MII/MIII-$(OH)_6$) stacked and present between the anions and water molecules arranged *via* hydrogen bonding and weak van der Waals force, the layered double hydroxide catalyst makes it possible for OER and HER to occur by providing a pathway and space for the electrolyte ions to come and intercalate. This is made possible thanks to the fact that the layered double hydroxide catalyst. The hydrophilic qualities can be amplified by including a higher proportion of water, and the interlayer distance can be modified by adjusting the proportions of cations to anions present in the compound. Cu now plays a more significant part in LDH systems as a direct consequence of the increased emphasis placed on OER, HER, and total water splitting (TWS). According to Yu *et al.*,[154] the production of Cu@CoFe LDH for TWS can be accomplished with little effort by employing either an electroreduction or an electrodeposition technique. Annealing the CuO@Cu foam that was produced after $Cu(OH)_2$ was grown on Cu foam was necessary to bring forth the material's full potential. The addition of electroreduction resulted in the creation of copper nanowires embedded in copper foam. The previously described core–shell nanoarchitectures were produced by the utilization of Co and Fe metal precursors during a subsequent cycle of electrodeposition. The effects of these catalysts on OER, HER, and TWS were investigated while they were in an aqueous solution containing 1 M KOH. OER polarization tests discovered that the activity of Cu@CoFe LDH was much higher when compared to that of Cu foam, Cu NWs at Cu foam, and CoFe LDH at Cu foam. This was the conclusion reached after comparing the three systems. The electrodeposited Cu@CoFe LDH samples that were put to the test showed that the 60 s sample had the maximum activity. This sample required an overpotential of just 240 mV to obtain a current density of 10 mA cm^{-2}. The relatively low Tafel slope value of 44.4 mV dec^{-1} is proof of the catalyst's quick charge transfer kinetics. The accuracy was verified by a chronopotentiometry study that lasted for 24 hours and found that there were no discernible changes in potential during the experiment. A Tafel slope value of 36.4 mV dec^{-1} is comparable to an overpotential of around 171 mV, which was required to create a current density in HER of 10 mA cm^{-2}; this was one of the requirements for the experiment. An investigation using chronoamperometry that lasted for 30 hours demonstrated the HER's activity and stability as a two-electrode system in a very basic environment. The HER's activity almost did not decrease at all over the course of the experiment, which indicates that the activity was very stable. An electrolyzer that used a Cu@CoFe LDH-60 as both the anode and cathode needed only 1.681 V to function, which is 60 mV higher than an electrolyzer that used an IrO_2 anode and a Pt cathode when the current density was 10 mA cm^{-2} (Fig. 7a). In this study, researcher perform a chronopotentiometry analysis on both systems at a current density of 10 mA cm^{-2} to investigate the stability requirements for Cu-based catalysts in a two-electrode set-up extreme. Stability was maintained with minimal degradation for up to 48 hours when Cu@CoFe LDH-60 was used as both the anode and cathode in the system; however, the overpotential in the IrO_2/Pt system rapidly increased after 12 hours of operation. Cu-based LDHs certainly show promise given that their predicted faradaic efficiencies are so close to reaching 100%. In addition to having a larger C_{dl} and a lower R_{ct}, it was found through computation that the C_{dl} in EIS

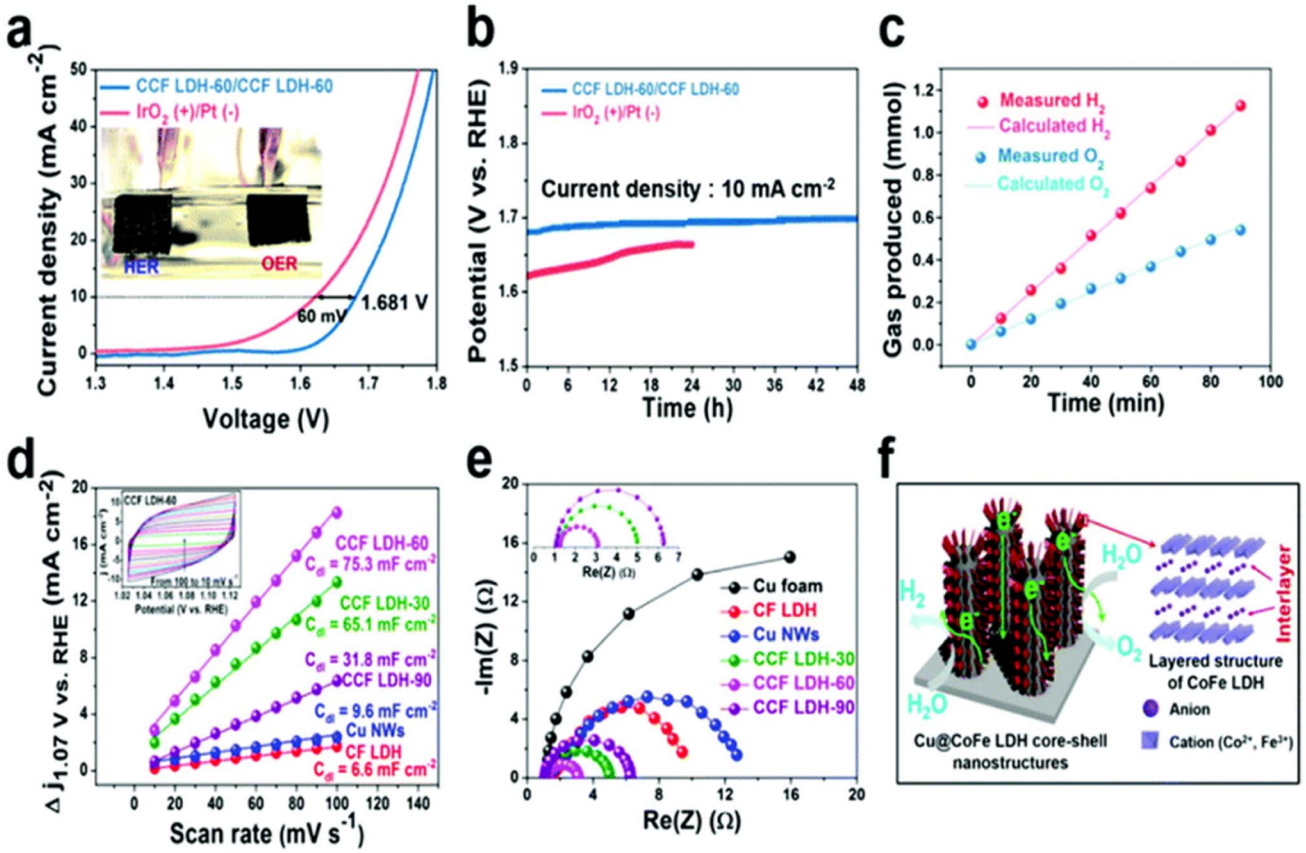

Fig. 7 (a) LSV, (b) GSTAT analysis, (c) faradaic efficiency, (d) ECSA, (e) Nyquist plot, and (f) the structure of Cu@CoFeLDH over Cu foam (reproduced with permission from Elsevier, copyright 2019).[154]

is more promising for prospective future uses. This finding comes after the discovery that the R_{ct} in EIS is lower (Fig. 7b–f). The significance of utilizing Cu-efficient TWS in an alkaline setting was demonstrated by this line of research, which validated its importance. Another observation made by the same group[155] concerned the use of Cu@NiFe LDH for TWS generation in 1 M KOH. In this illustration, the LDH structure was produced by depositing a highly active metal precursor, NiFe, on top of a Cu foam. The Cu foam served as the substrate for the LDH structure. To briefly recap, the Cu@NiFeLDH/Cu foam was manufactured using a process that included electroreduction as well as electrodeposition. The required overpotential for OER was 199 mV when the current density was 10 mA cm $^{-2}$, yet the Tafel slope value was only 27 mV dec^{-1}, indicating that approximately four electrons were transported at this current density. Overpotential for HER was measured to be 116 mV when 10 mA cm $^{-2}$ was applied, and the Tafel slope was 58.9 mV dec^{-1}. Both OER and HER exhibited a high degree of consistency with one another. The findings of the TWS showed that the Cu@NiFe LDH system only required 1.54 V between the anode and the cathode to attain 10 mA cm^{-2} current density, in contrast to the IrO_2/Pt system, which required 1.63 V between the anode and the cathode. The dependability of the Cu@NiFe LDH electrodes has been established using post-structural testing such as HRTEM, mapping, and XPS (Fig. 8a–e). The mapping research unearthed every feature that had been predicted to be there. During the process of reevaluating the stability of the polarization curves, evidence of OER and HER activity was found. A comparison of the OER and HER LSV curves reveals that the shifts that were found to have occurred were not particularly large (Fig. 8f). The results of these experiments, which compare LDH structures based on copper to those based on other transition metals, are positive since they open the way for the potential straightforward commercialization of these structures in the not-too-distant future.

Additionally, it was discovered that the OER activity of NiFe LDH that contained copper in the form of $Cu(OH)_2$ was boosted when it was mixed with potassium hydroxide. $Cu(OH)_2$@NiFe LDH was grown by Zhang *et al.*[20] on carbon paper by employing a modification of the unipolar pulse electrodeposition (UPED) technique. Adjustments were made to both the power consumption during deposition and the Ni/Fe feeding ratio. The OER activities of $Cu(OH)_2$ that had been deposited on NiFe LDH/CF were also investigated. Depositing $Cu(OH)_2$@NiFe LDH over carbon paper was accomplished using several techniques, including atomic layer precipitation evaporation deposition (UPED), cyclic voltammetry (CV), the potentiostatic method (PM), and the pulse potentiostatic method (PPPM) (PPM). The OER activity of each of these catalysts, which were produced by varying the stoichiometry and the amount of energy applied,

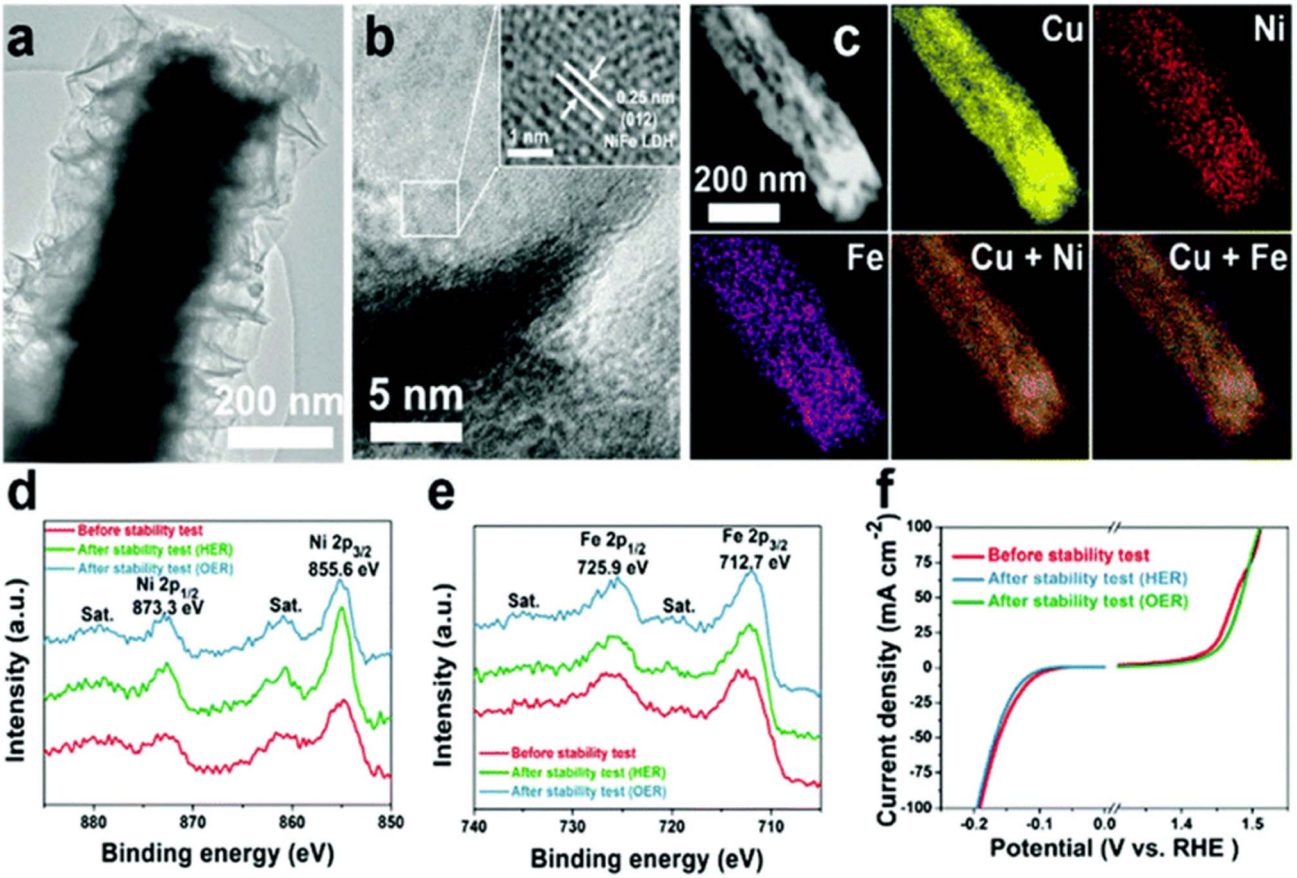

Fig. 8 (a and b) HRTEM images (c) mapping results, (d) Ni 2p XPS, (e) Fe 2p XPS, and (f) the structure of Cu@CoFeLDH over Cu foam (reproduced with permission from RSC, copyright 2017).[155]

has been investigated. During the deposition process, the OER activity connected to the consumption of 2.5 °C of energy was found to be greater than that seen for any other amount of power that was used. In addition, when the CV technique, the PM method, and the PPM method were compared to the UPED method, it was found that the UPED method was the most effective for depositing $Cu(OH)_2$@NiFe LDH. This was determined while comparing the UPED method to the CV method, the PM method, and the PPM method. The UPED method of testing revealed that a ratio of 6 : 4 Ni/Fe is optimal, with an overpotential of approximately 283 mV at a current density of 10 mA cm $^{-2}$ and a Tafel slope value of 88 mV dec^{-1} that is lower than that of all other materials, except for $Cu(OH)_2$ and NiFe LDH. These values were determined using a current density of 10 mA cm $^{-2}$. The benefits of combining NiFe LDH and $Cu(OH)_2$ were proved by the findings of a continuous electrolysis stability test that lasted for ten hours. After long-term, continuous electrolysis, only $Cu(OH)_2$ was degraded in the $Cu(OH)_2$@NiFe LDH reaction because NiFe LDH prevented $Cu(OH)_2$ from leaching. The OER and HER activities can be improved by mixing superstructures based on Cu with those based on Ni, Fe, and Co, all of which are transition metal LDHs. Copper, when combined with highly active Ni to produce NiCu LDH, has been the subject of intense research for its potential applications in OER. Following the production of NiCu LDH, the brucite layer was cleaned of Cu(II) by employing a straightforward ion-reductive complexation extraction (IRCE) technique.[156]

Ni-Cu_x LDH was developed as a solution to fill this void in the industry's requirements, and it catalyzed OER to produce exceptionally high levels of OER activity. NiCu LDH exhibits low levels of OER activity, just like $Ni(OH)_2$ does. Although the exfoliation process reduces the mechanical stability of LDH structures and, as a result, their OER activity, it has the potential to increase the activity of less active LDHs, such as NiCu LDH, by introducing flaws into the material. In this instance, the complexation of an ionic extractant led to the formation of vacancies rather than a change in the structure itself. The disruption of the transition metal based LDH structures is avoided because of this, which is a useful effect. An overpotential of approximately 343 mV is required to obtain 10 mA cm $^{-2}$ for OER when using only NiCu LDH. The development of vacancies in SAV-Ni-Cu_x LDH led to a reduction in the overpotential to 290 mV when the current density was 10 mA cm $^{-2}$. The Tafel slope for the NiCu LDH was 83 mV dec^{-1}, while for the SAV-Ni-Cu_x LDH, it was a much more manageable 45 mV dec^{-1}. Simply applying an overpotential of 355 mV was sufficient for the SAV-Ni-Cu_x LDH to achieve a current density of 100 mA cm^2. Since we now know how to produce LDHs utilizing

catalysts based on copper, we may employ vacancy engineering to significantly boost their activities for oxygen evolution reaction (OER) without changing the surface of the LDHs. In response to this challenge, researchers have developed unique techniques for creating highly active NiCu LDH nanostructures. One example of this is the modification of the synthesis technique. Zheng *et al.*[157] utilized a solvothermal growth method to successfully cultivate NiCu LDH directly on carbon fabric. A Tafel slope of 42.5 mA cm $^{-2}$ was achieved by using an overpotential of only 290 mV when the current density was 10 mA cm $^{-2}$. The results of the stability test offer further evidence that NiCu LDH for OER can be relied upon as a reliable reagent. According to the findings of the researchers, the OER activity of trimetallic LDH is significantly higher than that of bimetallic LDH.

Hu *et al.*[158] discuss the procedure of preparing N-doped NiZnCu LDH with rGO over Ni foam to carry out hybrid water electrolysis. This procedure is carried out on nickel foam. This study focuses on hybrid electrolysis ways to lessen the environmental impact of OER alone. Some examples of hybrid electrolysis approaches include ammonia electrolysis, urea electrolysis, and hydrazine electrolysis. Overpotentials of 460 mV were required for 100 mA cm $^{-2}$ in OER when utilizing N–NiZnCu LDH/rGO, but in HER, the same current density required overpotentials of 196 mV. Ni–Zn–Cu lyase/uridine dehydrogenase/glutamate (N–NiZnCu LDH/rGO) when we did a comparison using a configuration with two electrodes, we discovered that the voltage needed to reach 100 mA cm $^{-2}$ was 1.974 V. These findings demonstrated that trimetallic LDH systems, which utilized copper (Cu) as the transition metal, were successful in enhancing both OER and HER. It was discovered that the activities of Cu-based LDH catalysts for OER, HER, and TWS applications could be easily enriched by modifying the structures, method of synthesis, and direct growth over conducting substrates. Additionally, it was discovered that cationic vacancies could be created on the surfaces of LDHs using different methods without disrupting the LDHs' surface by using different methods. In addition, the stability of copper-based LDHs was demonstrated to be more obvious than the stability of copper-based oxides and hydroxides. The OER, HER, and in TWS study that involved long-term stability studies at high current densities for Cu-based LDH structures provided direct proof for these results. There is still the possibility of boosting LDH activity by modifying the copper-based surfaces of the organisms.

4.2. Cu-based sulfides for OER and HER

In HER and OER applications, as well as situations with a wide range of pH levels, a substantial amount of research has been carried out on the use of copper sulfides. By attaching protons to the surface of the HER at lower overpotentials, for instance, sulfides ions, which have a high degree of electronegativity, can boost the effectiveness of the HER. When it comes to electrocatalytic applications, the superionic conductivity of chalcogenide-based copper catalysts is highly sought. These

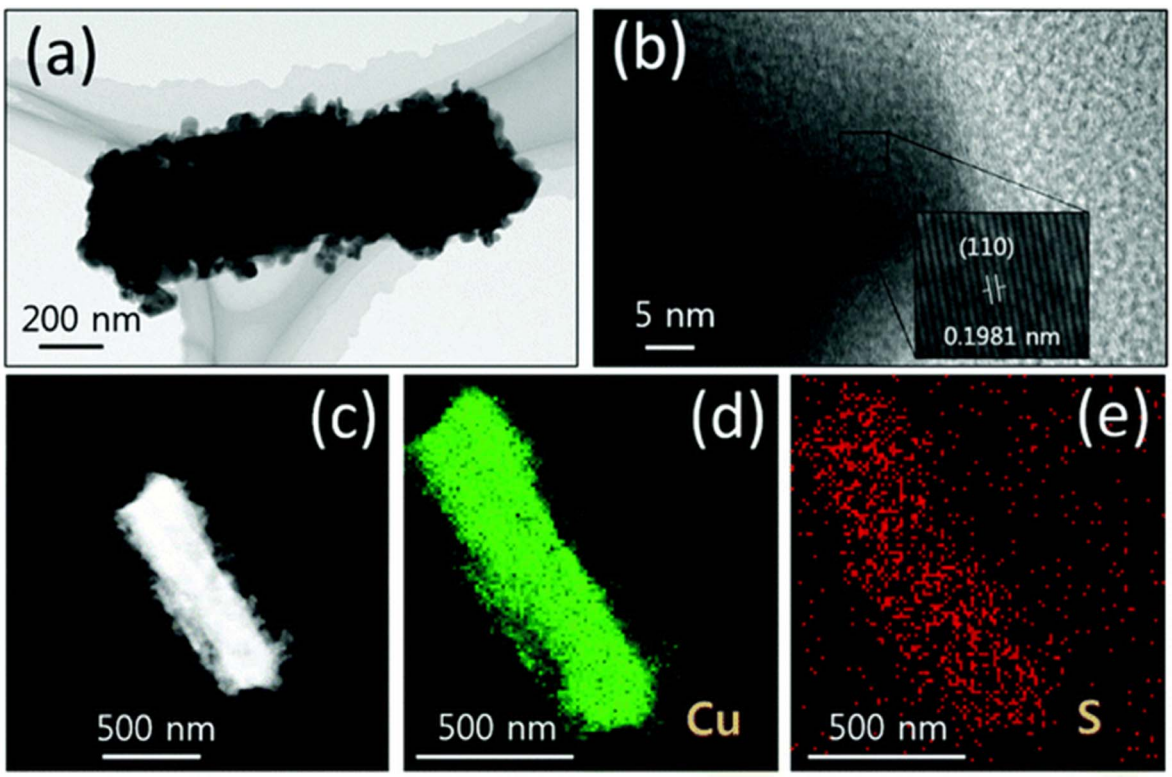

Fig. 9 (a–e) Cu_2S over the Cu based substrate HAADF mapping and HRTEM imaging (reproduced with permission from ACS Publications, copyright 2018).[159]

sulfide-based catalysts play the role of pre-catalysts. During the OER process, they either undergo oxidation to the oxide phase or reduction to the hydroxide phase, depending on the stoichiometry. In either case, they exhibit significantly increased activity in comparison to their bare oxide and hydroxide counterparts. As a result, researchers working in OER and HER have begun focusing their attention on materials based on chalcogenides. Working with sulfides of copper is in high demand for applications involving HER and OER because copper has a high conductivity, sulphur has various stoichiometries, and the compound tends to act as a pre-catalyst during these reactions. Oxygen evolution reactions (OER) were carried out in 1 M KOH with the use of Cu_2S nanorods that had been produced by employing a sacrificial template.[159] Because the (100) orientation is favored and the chain is increased with square planar coordination with OH ions, growing $Cu(OH)_2$ nanorods required first treating Cu substrates with $(NH_4)_2S_2O_8$ to generate $Cu(OH)_2$, which was a prerequisite for growing the nanorods. The sulfurization process was finished when the $Cu(OH)_2$–Cu substrate was left in the Na_2S solution for an extended period. This led to the formation of Cu_2S on top of the Cu substrate. Cu_2O was changed into Cu_2S since the solubility product of Cu_2S was lower than that of Cu_2O. Fig. 9a–e illustrates the morphological characteristic of nanorods, and the mapping demonstrates that copper and sulphur are dispersed evenly over the surface of the material. Cu_2S/Cu that was subjected to OER required just 270 mV as an overpotential to reach 10 mA cm^{-2} in current density. The needed overpotentials for $Cu(OH)_2$ were 390 mV, but for pure copper, the required overpotentials were 510 mV. Researcher discovered a rapid charge transfer kinetics in Cu_2S/Cu, which came in at 128 mV dec^{-1}.

The results of the chronopotentiometry investigation demonstrate that the current density of 10 mA cm^{-2} does not change (Fig. 10a–d). Using the ion exchange technique, a Cu_2S/Cu compound with a high activity level was easily generated. Sulfides can be incorporated into the inert structures that are based on CuO to boost their performance. In a solution of 1 M potassium hydroxide, Wang *et al.*[160] demonstrated the anodization-cum-hydrothermal synthesis of Cu_2S nanorods over Cu foam for OER. Cu_2O nanowires were formed when the copper foam was anodized in potassium hydroxide (KOH) and then annealed afterward. The production of Cu_2S nanoarrays

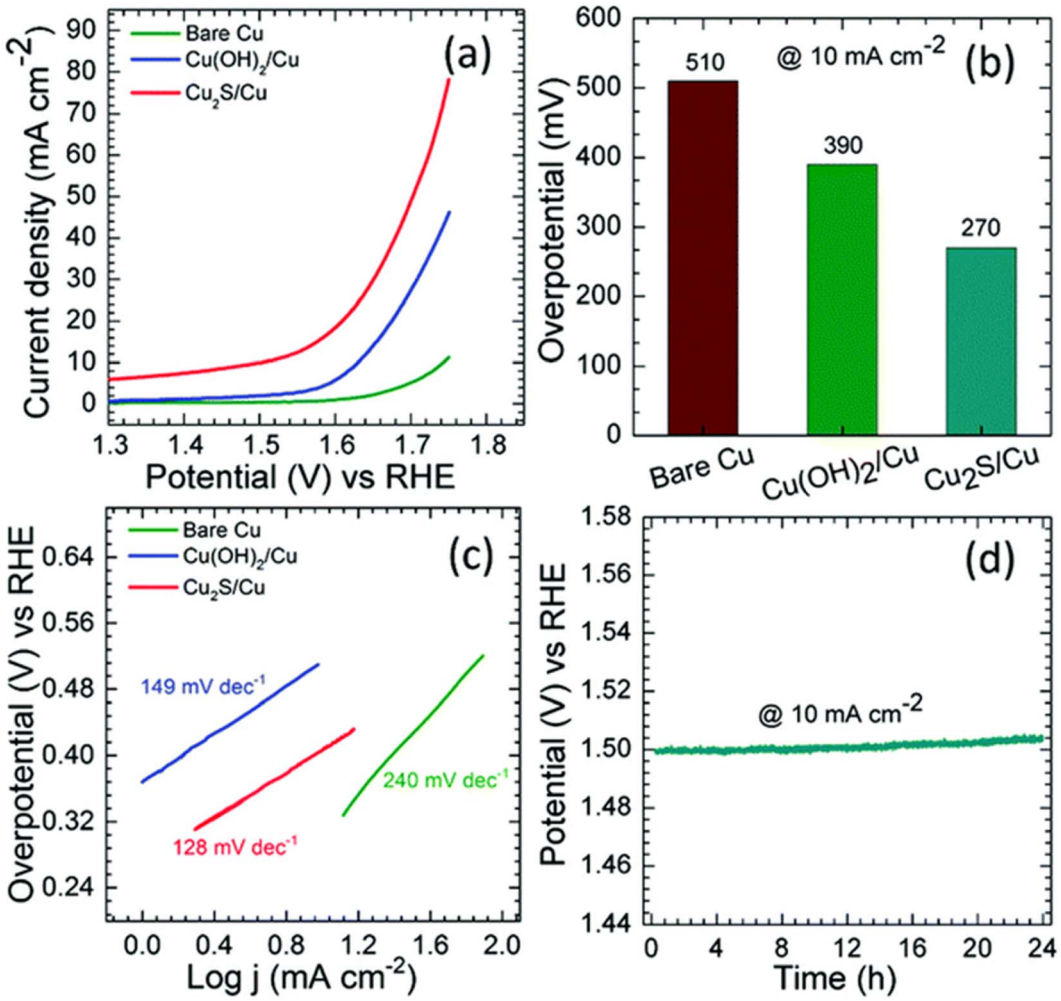

Fig. 10 (a–d) showing LSV, overpotential at 10 mA cm^{-2}, Tafel slope, and chronopotentiometry respectively (reproduced with permission from RSC, copyright 2020).[159]

was accomplished by adding thiourea to a solution that was subsequently subjected to hydrothermal processing. Using thiourea in one of three different concentrations resulted in the production of Cu_2S-NA/Cu foams that were somewhat different from one another. The Cu_2S-NA/Cu foam-50 displayed the highest level of OER activity; to maintain a current density of 50 mA cm^{-2}, an overpotential of 360 mV was necessary. At 75 mV dec^{-1}, the slope of the Tafel was not as steep as it would normally be.

With a reaction time of only 5 minutes, He *et al.*[161] highlighted the quickest approach for the sulfurization of 3D Cu foam to Cu_2S nanosheets arrays *via* plasma treatment and with the severe anion exchange. This was accomplished by converting the foam into nanosheets. At an overpotential of only 336 mV, the OER activity of Cu_2S/CF in 1 M KOH was seen to reach a value of 20 mA cm^{-2} at its maximum. The comparison of the active surface area produced with the sulfurization technique by plasma treatment for CuI/CF and Cu_2S/CF with ECSA showed that there was a significant gap between the two values, with the former measuring 25.3 mF and the latter measuring 160.7 mF. In addition to this, the R_{ct} difference demonstrates that CuI/CF has significantly higher values than Cu_2S/CF, which provides additional evidence that the sulfurization process was successful (Fig. 11a–d). Changing the structure of CuS (covellite) to Cu_2S (chalcocite) was used in the research[162] to investigate OER activity in phosphate buffer solution.

In this instance, the conversion of CuS to Cu_2S was accomplished, and the addition of glycine led to an even greater rise in OER activity. The OER performance can be improved by lowering the concentration of CuS and Cu_2S to create a phase shift. This is because CuS and Cu_2S are semiconductors due to the presence of Cu vacancies in the lattice. The CuS phase transition was analyzed, and the results showed van der Waals layers as well as S–CuS_3–Cu–CuS_3 layers running along the c-axis. The presence of OAm was beneficial to the reduction process, and studies made on the planes (001) and (110) of CuS and Cu_2S revealed that the S atoms were tightly packed in a hexagonal configuration. The primary distinction lies in the fact that Cu_2S chalcocite formations contain an additional Cu cation that is injected into the spaces that exist between the S sites. To ascertain the OER of these Cu_2S NPs, they were tested in a solution that comprised 6 mM of glycine and 250 mM of phosphate buffer. This concentration of glycine was shown to be particularly beneficial when compared to the increases in activity that were observed with other doses and additions. Both the initial potential of the OER, which is approximately 272 mV, and its overpotential at 10 mA cm^{-2}, which is 428 mV, are lower when compared to the overpotential of CuS, which is 586 mV. In this article, researcher take a detailed look at how the OER activity of copper-based sulphides can be increased by using phase transformation in conjunction with glycine. The exceptional activity and stability of these copper-based sulphides catalysts attracted the attention of scientists working in the field

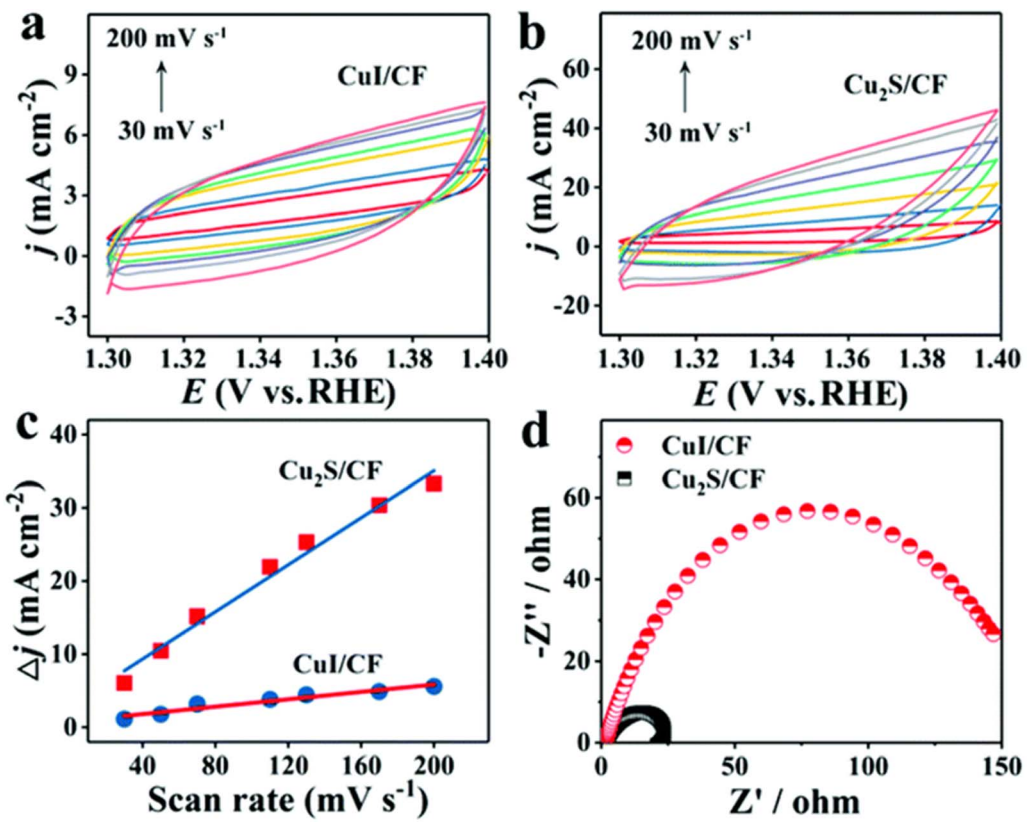

Fig. 11 (a–c) determination of ECSA for non-faradic region for CdI and (d) the EIS (reproduced with permission from ACS Publications, copyright 2018).[161]

of heterogeneous catalysis (HER). Bhat *et al.* used Cu_2S micro-hexagons that were produced hydrothermally for HER at two different pH levels, pH = 0 and pH = 14. Both pH values were very different. In alkaline conditions, current densities of 10 mA cm^{-2} may be reached at an overpotential of 330 mV, but in acidic conditions, the necessary overpotential is 312 mV.[163] Potentiostatic and potential-dynamic stability experiments indicated that Cu_2S micro-hexagons are exceptionally stable, demonstrating that Cu_2S can tolerate harsh pH conditions and can be employed in HERs. This is another indication that Cu_2S can be utilized in HERs. It is possible to improve the HER's kinetics by include sulphides that are based on transition metals other than copper in the reaction. Wang *et al.*[164] presented evidence that HER may be manufactured by layering Cu_2S and MoS_2 on top of a Cu foam substrate.

The Cu_2S/MoS_2/Cu foam was produced through the hydrothermal addition of thiourea and sodium molybdate, which was then followed by the formation of $Cu(OH)_2$ over the Cu foam. Through the utilization of thiourea, N-doping of MoS_2 was successfully accomplished. Using a Cu_2S/MoS_2/CF electrode, KOH HER testing demonstrated an overpotential of 91 mV when the current density was 10 mA cm^{-2}. Current densities of 100 mA cm^{-2} were achieved with an overpotential of only 129 mV. When compared to the activity of Cu_2S/CF, the activity of Cu_2S/MoS_2/CF is significantly higher. The fact that Cu_2S/MoS_2/CF has a Tafel slope of 41 mV dec^{-1} suggests that it is relatively stable. There have been reports of these copper sulphides being used in applications involving OER and HER, particularly in combination with other catalysts based on transition metals. At ambient temperature, Cu_2S nanorods encased in CoS shells were created by combining $Cu(OH)_2$ NRs/CF and $Cu(OH)_2$ NRs@$Co_2CO_3(OH)_2$/CF as in Fig. 12.[165] Experiments involving OER and HER were carried out in 1 M KOH using the catalysts that had been created. The additive action of copper sulphate (Cu_2S) and cobalt sulphate (CoS) resulted in increased OER and HER activity in alkaline media. OER was achieved with a relatively low overpotential of 275 mV at 50 mA cm^{-2} in the instance of Cu_2S NRs at CoS/CF. The kinetics of charge transfer are likewise quite fast; the Tafel slope is only 54 mV dec^{-1}. A current density of 50 mA cm^{-2} was achieved by Cu_2S NRs@CoS/CF, which is comparable to that of HER. The overpotential of Cu_2S NRs@CoS/CF was 324 mV, and the Tafel slope for charge transfer kinetics was 121 mV dec^{-1}. In alkaline electrolyte, OER and HER composites of Cu_2S and CoS using conductive Cu foam as the 3D support were extraordinarily stable. The improvement in activity for OER and HER based-on copper sulphides can be attributed to several factors, including the use of conducting 3D networks like Cu foam, the growth of hydroxides to sulphides *via* several different routes, the occurrence of a phase transformation, the addition of sulfur, and the incorporation of other transition metal sulfide-based materials into the composition. Other factors include the use of conducting 3D networks like Cu foam; the on the other hand, as

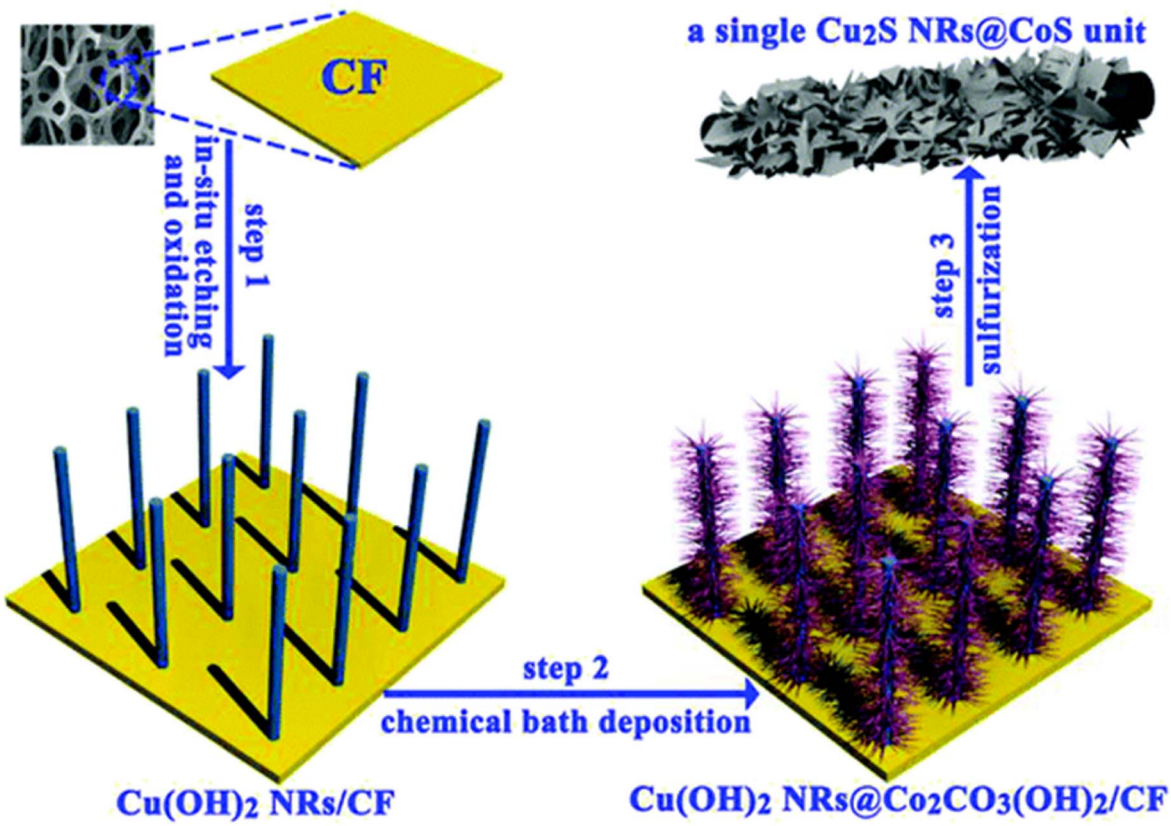

Fig. 12 Process description of CoS-shelled Cu_2S nanorods over Cu foam (reproduced with permission from Elsevier, copyright 2019).[165]

was previously demonstrated, copper sulphides are both a more active and stable substance than copper oxides.

4.3. Cu-based selenides for OER and HER

Copper selenides are highly conductive materials, in addition to having positive impacts on both OER and HER. There is a significant body of research suggesting that selenides derived from copper exert potent HER and OER effects. Wang *et al.*[166] report utilizing copper oxide synthesized from copper selenide to increase OER in 1 M KOH. At this location, Cu_2Se/Cu foam was produced through the reaction of $Cu(OH)_2$/CF with $NaBH_4$ and Se while the reaction was carried out at room temperature. Because of this, copper oxides formed on the surface of the Cu_2Se/Cu foam because of electrochemical oxidation. When tested in 1 M KOH, the OER activity of this catalyst was significantly higher than that of $Cu(OH)_2$ or CuO/CF. When compared to CuO–C and $Cu(OH)_2$, CuO–A/CF exhibited significantly higher activity and only needed an overpotential of 297 mV to obtain 10 mA cm^{-2}, but CuO–C and $Cu(OH)_2$ did not. In a Tafel investigation, the low result of 72.8 mV dec^{-1} for CuO–A/CF is indicative of how easily charge may be transferred from one substance to another. The stability was further supported by research that utilized galvanostatic techniques, which demonstrated that there was no decrease in activity after 50 hours had passed since the reaction began. When compared to the properties of other materials, CuO–A/CF possesses superior ECSA and R_{ct} values (Fig. 13a–f). This study provides evidence for the significance of the production of on-site $Cu(OH)_2$ surface oxide in the enhancement of copper-based selenides in OER. Cu_2Se/CF was demonstrated and used for OER in 1 M KOH by Shi *et al.*,[167] who utilized the solution immersion method to conduct their experiments. Researcher immersed the pretreatment Cu foam in a solution containing $NaBH_4$ and Se so that could build and test several different catalysts for OER. Several different lengths of time were spent subjecting the foam to copper precursors as well as selenide. The Cu_2Se/OER CFs are only 10 mA cm^{-2} at only 200 mV overpotential, which is a substantial reduction compared to those of other selenide-based catalysts. The observed value of the Tafel slope was 62.4 mV dec^{-1}, in addition to being lower than the value predicted. The low activity of metallic and hydroxide compounds is shown by the fact that Cu_2Se/CF is more active than either bare CF or $Cu(OH)_2$/CF. This demonstrates that metallic and hydroxide compounds have a low activity level. It's possible that the formation of a surface oxide was responsible for the blackening of the electrode that occurred during the Cu_2Se/CF OER research. This demonstrates that the oxide phase that is generated during OER is the active catalyst, whereas the copper-based selenide catalysts just play a pre-catalytic function in the process. Copper selenides prepared by chemical vapor deposition (CVD), electrodeposition (ED), and hydrothermal techniques were put to the test by Masud *et al.*[168] to determine their suitability for usage in organic electron receptors.

All the techniques were able to successfully synthesize Cu_2Se and test it for its OER content in 1 M KOH. The Cu_2Se material was discovered to be the most effective and long-lasting substance in the trials that were analyzed. At an overpotential of 270 mV and a current density of 10 mA cm^{-2}, simple OER activity was found in the electrodeposited sample. Based on these data, it appears that the intrinsic catalytic activity of a medication, rather than the process by which it was synthesized, is the factor that determines the activity of the drug. The

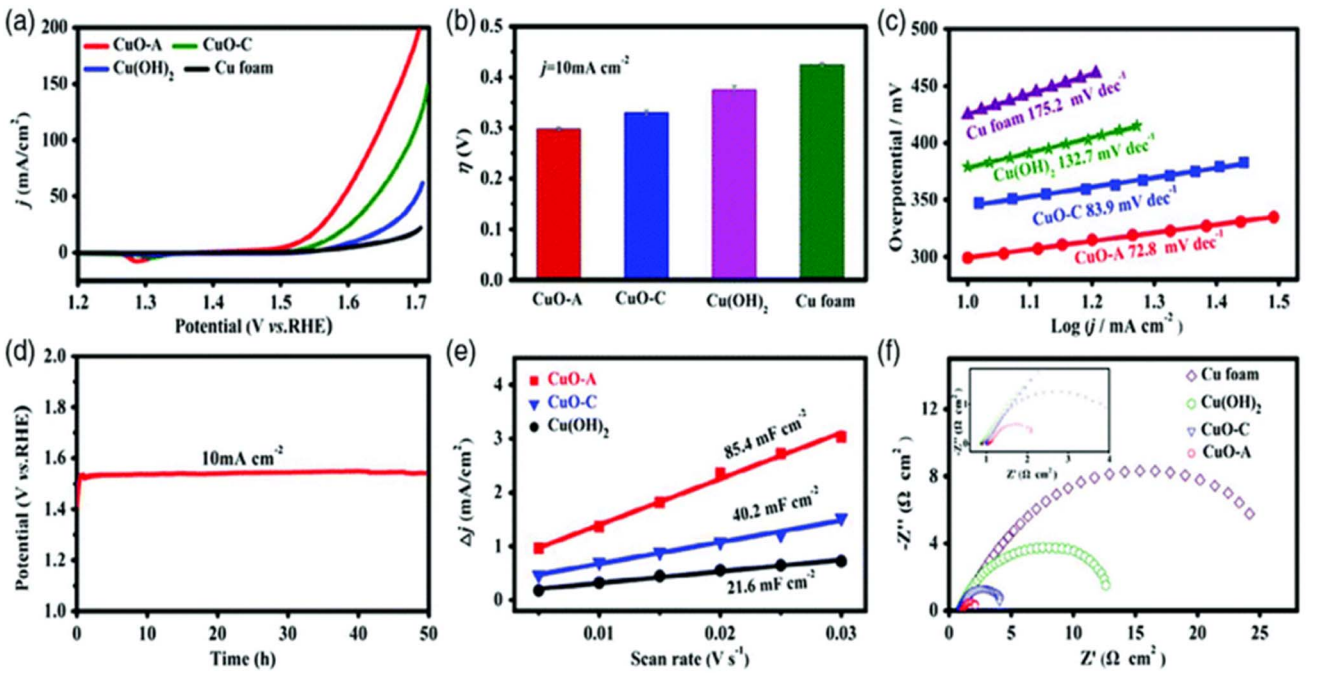

Fig. 13 (a–f) LSV, overpotential at 10 mA cm^{-2}, Tafel slope, chronopotentiometry, ECSA, and EIS results of CuO–A, CuO–C, and $Cu(OH)_2$ (reproduced with permission from ACS publications, copyright 2018).[168]

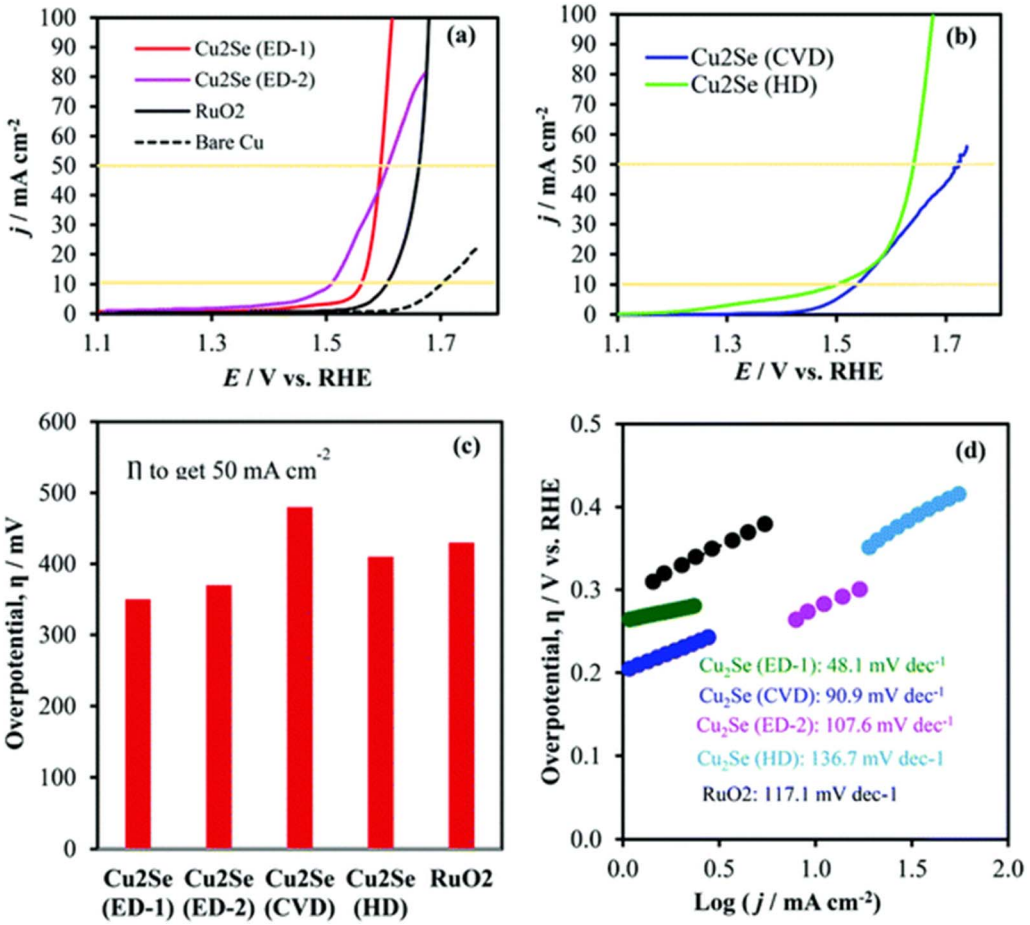

Fig. 14 (a) and (b) LSV, (c) overpotential at 50 mA cm $^{-2}$, and (d) the Tafel slope results of Cu_2Se catalysts (reproduced with permission from ACS publications, copyright 2018).[168]

sample that was electrodeposited demonstrates a high rate of charge transfer kinetics (48.1 mV dec^{-1}). In addition, the polarization study demonstrated that there was very little to no variation in activity once stability was proven. This ensured the use of Cu-based selenides for OER in an alkaline environment, and the chronoamperometry analysis confirmed the durability of the selenides. Both studies can be found here (Fig. 14a–d). Copper selenides, thanks to the combination of their conducting copper support and the electronegative se, were discovered to be towards the top of the HER material hierarchy by the researchers. This was since copper selenides have the potential to successfully incorporate H^+ ions. Because of this, there is a strong demand for copper-based selenides in applications involving HER. As was said earlier, salinization may take place over the Cu foam if the initial conversion of copper to $Cu(OH)_2$ is effective, and the salinization process is then carried out utilizing the precursors sodium bisulfite and selenium. Zhang *et al.* utilized an *in situ* anion exchange technique to prepare $Cu_{2x}Se$/CF. Specifically, they exchanged the OH ions from $Cu(OH)_2$/CF for the Se ions formed when $NaBH_4$ reacts with Se. This allowed them to produce $Cu_{2x}Se$/CF.

Acid treatment was then performed on $Cu_{2x}Se$/CF so that it could be used in HER applications. An overpotential of only 313 mV was required to achieve the desired current density of 100 mA cm^{-2} in the circuit. Tafel slopes of 90.77 mV dec^{-1} and 84.4 mV dec^{-1} were obtained from studies of $Cu_{2x}Se$/CF conducted using CV and log $R_{ct}1$, respectively. Even in an acidic environment, the findings indicate that cathodic current densities of 50 mA cm^{-2} for 24 hours are relatively stable. This study provides support for research that is being conducted in the field of HER since it demonstrates the high activity and stability of copper-based selenides in acidic conditions. After utilizing a hydrothermal method to selenize the material, Anantharaj *et al.*[169] noticed a reduction in the high overpotential need with Cu foam of up to 1 V. This was the result of the selenization. The hydrothermal and wet–chemical processes were used to treat the copper foam using $NaBH_4$ and Se. To evaluate the HER activity of the synthesized catalysts, a 0.5 M H_2SO_4 solution was applied to the catalysts. Selenization of copper by itself was sufficient to bring the overpotential down by a significant amount in this case. It was possible to achieve kinetics comparable to those of Pt/C-based catalysts in HER because the charge transfer resistance was about 0.3–0.6 and the Tafel slope values were nearly 32–35 mV dec^{-1}. There was also further evidence that confirmed the consistency of the results.

4.4. Cu-based phosphides for OER and HER

Because of its high electrical conductivity and metalloid composition, the metalloid copper phosphide has been the focus of substantial research for electrocatalytic water splitting. Synergistic increase of the OER is observed while utilizing transition metal catalysts based on phosphide compounds. In addition, the phosphide (P_3) ions that make up HER can swiftly and efficiently bind protons. Tian *et al.*[170] demonstrated that copper foam may be used well as an electrode for HER in acidic environments. These researchers demonstrated that it is possible to generate arrays of Cu_3P nanowires directly on top of the foam. Since Cu and the pendant base P were so effective at catalyzing the reaction, it was determined that they are to blame for the increased HER activity. The benchmark for this experiment was microparticles composed of the substance Cu_3P. Cu_3P NA/CF had an attenuation threshold of 62 mV when subjected to a current density of 10 mA cm $^{-2}$, whereas Cu_3P MP/CF had a threshold of 190 mV. Cu_3P NA/CF required just 67 mV dec^{-1} to enhance electron transport, but Cu_3P MP/CF required 96 mV dec^{-1} to accomplish the same goal. These findings demonstrate that HER nanostructures that include many active sites and can be accessed electrochemically are extremely useful. According to the findings of the rate stability investigation, the Cu_3P-based catalysts were extremely stable, with the LSV curve indicating nearly little activity loss after multiple cycles. It is possible to boost the HER activity of these phosphides based on copper by adding in other phosphides based on transition metals. According to the results of an intriguing study conducted by Chu *et al.*,[171] $Ni_{2x}Cu_x$-P nanosheets were utilized to increase HER activity in an alkaline medium.

The development of NiCu LDH on top of Ni foam was part of the work that was done here, and the resulting $Ni_{2x}Cu_x$-P/NF was use in HER applications once it was phosphorated as shown in Fig. 15. The HER of the NiCu LDH was improved thanks to an overpotential that was 136 mV. Overpotentials of 103 mV were necessary for Ni_2P, whereas 117 mV were necessary for Cu_3P. Phosphorization, as was the case before, demonstrates an improvement in activity compared to NiCu LDH. To produce $Ni_{2x}Cu_x$-P/NF, we altered the atomic ratio of Ni to Cu. $Ni_{1.8}Cu_{0.8}P$/NF had the highest level of activity among them, needing only 78 mV of overpotential to generate 10 mA cm^{-2} of current. In addition, in comparison to NiCu LDH and monometallic phosphides, the observed Tafel slope has been found to be a significant amount flatter at 70 mV dec^{-1}. Despite being subjected to a cycle study, the bimetallic phosphides did not appear to have undergone any major changes. In this scenario, Cu modifies the Fermi level to facilitate H_2 desorption.

These findings imply that the activity of HER might be further improved by modifying the stoichiometry, and that $Ni_{2x}Cu_x$-P/NF could benefit from the addition of a variety of transition metals as catalysts for HER. It will be interesting to see if the TWS can be applied to Cu-based phosphides to obtain a reduction in the overpotentials for OER and HER. Most of the research into OER and HER has focused on other transition metal-based phosphides, such as Ni and Co, so it will be interesting to see if the TWS can be applied to Cu-based phosphides. Hydrothermal treatment, followed by high temperature phosphorus conversion, was the method that Han *et al.*[172] used to synthesize Cu_3P/NF. To achieve OER using Cu_3P/NF, we needed an overpotential of 320 mV at 10 mA cm^{-2} and a Tafel slope of 54 mV dec^{-1} in 1 M KOH. The slope of the Tafel chart was around 42 mV dec^{-1}, and the required overpotential for HER was 105 mV. Because of Cu_3P/high NF's OER and HER activity, TWS has chosen to use it as both the anode and the cathode in their TWS reactor. It was possible to achieve a current density of 10 mA cm^{-2} at an overvoltage of 1.67 V, which is equivalent to an overpotential of only 440 mV. In addition, the initial overpotential for TWS using Cu_3P/NF

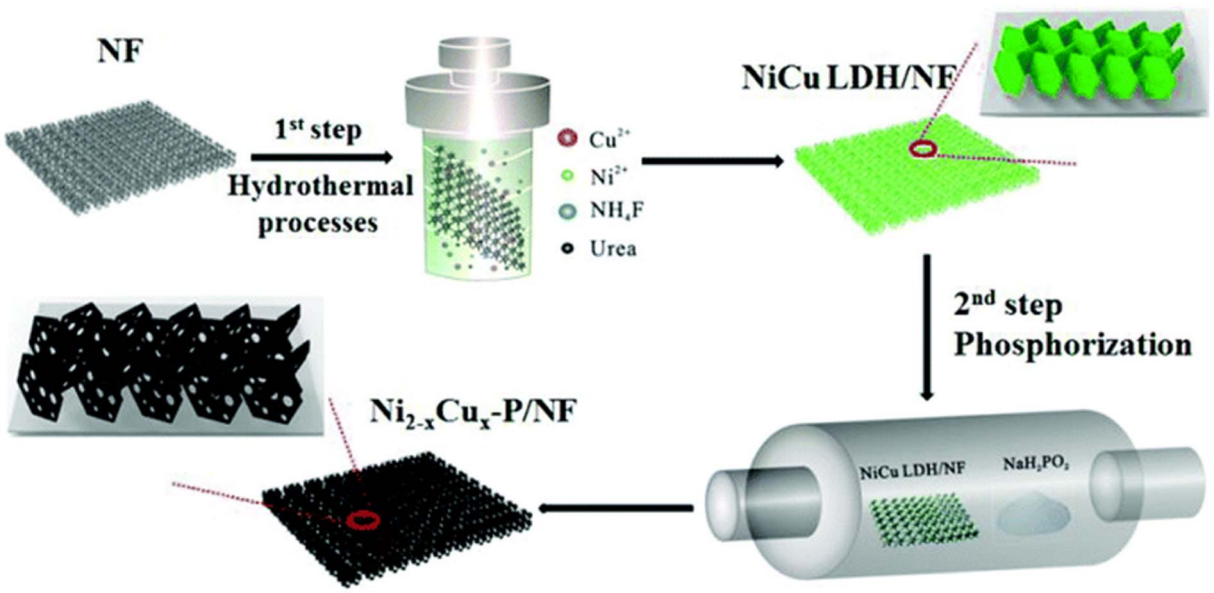

Fig. 15 Preparation of NiCu phosphide over NF for HER reaction (reproduced with permission from ACS publications, copyright 2017).[172]

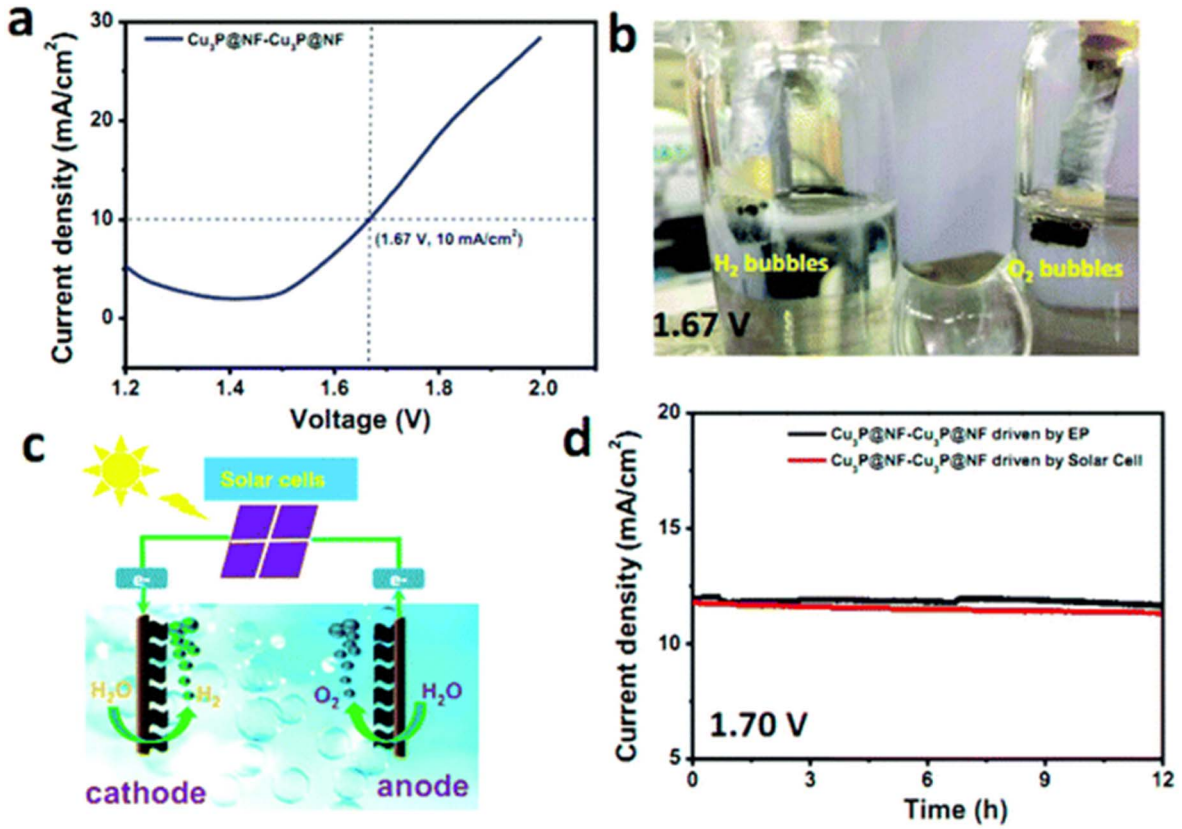

Fig. 16 (a–d) LSV, Cu_3P catalysts in KOH for two-electrodes, the scheme, and PSTAT analysis for 12 h (reproduced with permission).[172]

electrodes was only 270 mV, which is a relatively low value (Fig. 16a–d). After 10 hours of bulk electrolysis, Cu_3P/reliability NFs in industrial water splitting were also validated. As a direct consequence of these findings, Cu_3P has been investigated for its potential application as a stand-in for several transition metal-based catalysts, such as Ni and Co. When searching for precious metals to replace, copper phosphides provide the impression of being a promising alternative to other potential replacements. They are also resistant to breakdown in settings that are both acidic and alkaline, which adds to the possibility that they could be used as alternatives. It's possible that in the future, TWS with copper-based catalysts will be the way to go for making the most of limited resources. These phosphides based on copper can be utilized either on their own or in conjunction with other catalysts based on transition metals.

Cu-based tellurides have not been investigated as thoroughly as sulphides and selenides. The formation of $Cu_{2x}Te$ catalysts for HER in acidic electrolyte has been emphasized by Kumaravel *et al.*[173] $Cu_{2x}Te$ catalysts were produced using wet-chemical and hydrothermal methods, and their activities were compared. Hydrothermal production of $Cu_{2x}Te$ from Cu metal precursors in the presence of $NaBH_4$ and Te salts was achieved for the first time at room temperature. The homogeneous distribution of Cu and Te is supported by the observed HAADF mapping model. However, oxide generation cannot be prevented, which may dampen the potential in HER study. The effectiveness and longevity of telluride-based Cu was then investigated by HER. Compared to $Cu_{2x}Te$/WC, which required 432 mV to get the same current density, the generated $Cu_{2x}Te$/hybrid demonstrated significant activity by achieving an overpotential of 347 mV (HER performance is amazing). The larger prevalence of the facile charge transfer phenomenon in $Cu_{2x}Te$/hybrid is also indicated by the larger value of the Tafel slope, which is 188 mV dec^{-1}. Computational studies of electron impact spectroscopy (EIS) and electron correlation spectroscopy (ECS) revealed that the larger exposed active surface area of $Cu_{2x}Te$/substantially hybrid promoted faster electron transfer kinetics. In addition, potentiostatic analysis was utilized to measure the stability, and it was determined to be rather high for 12 hours with no variation in activity. This study employed a variety of synthetic methods to show that tellurides based on copper are necessary for evaporation control. As we have shown in our studies of Cu-based selenides, the activities of these Cu-based tellurides can be further improved by using conducting supports, expanding over 3D structures, increasing the metallic sites, and extending with other transition metal-based tellurides. For both OER and HER, it is highly desirable to develop Cu -based tellurides as a means of lowering energy inputs. Majhi *et al.*[174] investigated the HER of hydrothermally produced $CoTe_2$@CuTe and $FeTe_2$@CuTe nanocomposites in acidic, alkaline, and neutral electrolytes. The $CoTe_2$@CuTe catalyst required only 58.1 mV of overpotential for the HER studies conducted under acidic conditions, while the $FeTe_2$@CuTe catalyst required 86 mV. When compared to selenides ($CoSe_2$@ $CuSe_2$ and $FeSe_2$@

Table 3 Comparison of different Cu-based Catalysts for OER and HER

Sr. no.	Catalyst hybrid	Medium and study type	Tafel slope (mV dec^{-1})	Overpotential (10 mA cm^{-2})	References
1	Nanowires CuO	KOH (1 M) OER study	61.4	430	179
2	Bundles of CuO nanosheet	KOH (1 M) OER study	59	350	180
3	Nanosheet of CuO	KOH (1 M) OER study	135	320	181
4	Nanotubes of CuO	KOH (1 M) OER study	149	320	181
5	NPs/CuO	NaOH (1 M) OER study	64	290	182
6	Nano leaves of CuO	KOH (1 M) OER study	106	280	181
7	C/CF hybrid of CuO/HS	KOH (1 M) OER study	66.3	286	183
8	CF/CuSe	KOH (1 M) OER study	150	200	167
9	CF/Cu_2Se–A	KOH (1 M) OER study	72.8	297	166
10	NF/CuSe	KOH (1 M) TWS study	—	450	184
11	NF/Cu_3P	KOH (1 M) TWS study	—	440	172
12	NF/Cu_3P	KOH (1 M) OER study	54	320	172
13	CuTe/$CoTe_2$	PBS (1 M) OER study	67.6	106	174
14	NF/CuSe	KOH (1 M) OER study	128	162	168
15	NF/CuSe	KOH (1 M) OER study	89	297	168
16	LDH/NiFe/Cu	KOH (1 M) TWS study	—	310	185
17	LDH/NiFe/Cu	KOH (1 M) OER study	27.8	199	155
18	CoFe/Cu LDH	KOH (1 M) TWS study	—	451	154
19	CoFe/Cu LDH	KOH (1 M) OER study	44.4	240	154
20	Nanorods of Cu_2S	KOH (1 M) OER study	128	270	186
21	CC/LDH of NiCu	KOH (1 M) OER study	42.5	290	157
22	CF/NA-50 Cu_2S	KOH (1 M) OER study	75	360	160
23	Cu_2S–TiO_2–Cu_2S	KOH (1 M) OER study	72	284	180
24	Nanoflowers of CuO	KOH (1 M) OER study	270	84	181
25	CF/CuO–C–HS	KOH (1 M) OER study	134	299	187
26	FTO/CuO	Buffer of phosphate (0.2 M) OER study	57	500	188
27	Micro hexagons of Cu_2S	KOH (1 M) OER study	106	330	163
28	NPs/Cu–O_x–Ni	Na_2CO_3 (1 M) OER study	120	320	189
29	Cu–O_x–Ni/SAV	KOH (1 M) OER study	45	290	156
30	NiFe/$Cu(OH)_2$	KOH (1 M) OER study	88	283	185
31	Foam of Cu/Cu_3Sn	KOH (1 M) OER study	177	384	184
31	Cu_2S/CoS/NRs/CF	KOH (1 M) OER study	54	275	165
32	P/$Cu_{0.2}$/$Ni_{1.8}$	KOH (1 M) HER study	70	78	171
33	CF/rGO/CuO–Cu_2O/Cu	KOH (1 M) HER study	12	105	190
34	CuO/CO_3O_4	KOH (1 M) HER study	14	288	153
35	MoS_2O/Cu_2S	KOH (1 M) HER study	31	91	164
36	CF/Cu_3P	H_2SO_4 (0.5 M) HER study	67	143	170
38	Cu/CoFe	KOH (1 M) HER study	16	171	154
39	Micro hexagons of Cu_2S	KOH (1 M) HER study	28	312	163
40	CF/CoS/NRs Cu_2S	KOH (1 M) HER study	30	235	165
41	CuTe/$CuTe_2$	KOH (1 M) HER study	70	125.8	174
42	CuTe/$CuTe_2$	H_2SO_4 (0.5 M) HER study	60	68	174
43	$Cu_{2-x}Te$	H_2SO_4 (0.5 M) HER study	39	347	173
44	Poly polished Cu	KOH (1 M) HER study	13	320	151
45	NiFe/LDH Cu	KOH (1 M) HER study	19	116	185
46	CF/Cu_2Se	H_2SO_4 (0.5 M) HER study	35	212	169

$CuSe_2$), the overpotential was still quite high at 117 and 127.7 mV. As a result, tellurides based on copper and other transition metals had a more significant effect on HER than their selenide counterparts. In a similar vein, the overpotential required by $CoTe_2$@CuTe was 125 mV, whereas it was 203 mV for $FeTe_2$@CuTe at the same current density in neutral circumstances. Again, selenide analogues required far greater overpotentials compared to their telluride counterparts (225 and 252 mV, respectively). $CoTe_2$@CuTe and $FeTe_2$@CuTe required overpotentials of 106 mV and 122 mV at 10 mA cm^{-2}, respectively, in alkaline conditions; equivalent selenides required overpotentials of 129 mV and 180 mV, respectively. The prolonged activity with $CoTe_2$@CuTe and $FeTe_2$@CuTe is due to their high ECSA and BET surface area in comparison to the selenides, and their activities are consistent with those of the tellurides at pH 0, 7, and 14. Further, tellurides based on Co, Cu, and Fe have synergy that is competitive with selenides; hence, they are actively sought after for use in future HER applications. Nanocomposites of Cu-based tellurides with both Co and Fe have been the subject of much research, resulting in unprecedented activity and stability. In the future, this Cu-based telluride can be coupled with other transition metal-based tellurides to boost their activity in HER applications that work in acidic settings.

4.5. Ru modified Cu-BTC

A carbon skeleton was created by pyrolyzing a Ru-modified Cu-BTC precursor in N_2. This carbon skeleton enclosed bigger Cu nanoparticles as well as ultrasmall Ru nanoparticles (henceforth termed as S-0). Some of the Ru nanoparticles were converted into RuO_2 through a process called annealing, which was carried out in air. It was confirmed that the CuO nanoparticles lacked catalytic activity for HER and OER by etching them with three times the concentration of hydrochloric acid. In the end, researcher was able to procure the Ru/Cu-doped RuO_2 catalyst that was needed to perform the water splitting reaction. The overall performance of the water splitting electrocatalyst is superior to that of state-of-the-art electrocatalysts. To attain current densities of 10 and 100 mA cm^{-2}, respectively, only 1.47 and 1.67 V are required. According to the findings of the DFT study, doping RuO_2 with Cu has the potential to increase its OER performance. This is because it enables fine-tuning of the d-band center, which, in turn, modifies the electronic structure of the Ru activity sites on the RuO_2 (110) plane.[175]

4.6. Channel rich RuCu nanosheets

Researcher were able to construct channel rich RuCu nanosheets by using a wet chemical approach. These nanosheets are formed of crystalline Ru and amorphous Cu, and they feature many channels that may be accessed (denoted as RuCu NSs). The electrochemical performance of the optimized RuCu NSs is significantly higher when contrasted with that of their OER and HER counterparts. The RuCu NSs/C that were optimized at 350 °C showed activity that is desired for OER, while the RuCu NSs/C that were optimized for 250 °C showed activity that is desirable for HER. In water splitting applications utilizing the enhanced RuCu NSs/C, 10 mA cm^2 is reached at 1.48 V, 1.55 V, 1.49 V, and 1.50 V, respectively, in 1 M, 0.1 M KOH, 0.5 M, and 0.05 M H_2SO_4, when compared to those applications utilizing the RuCu NPs/C and commercial Ir/C||Pt/C. These voltages are attained in 1 M, 0.1 M, 0.05 M KOH, and after being subjected to long-term dependability tests, the optimized electrolyzer has been shown to maintain a steady overpotential with very little variation because of the tests' findings.[176]

4.7. Ru-doped Cu electrocatalysts

To make a Ru–Cu@C-1 sample, a RuCu-BTC-1 precursor was annealed at 500 °C for three hours in nitrogen at a heating rate of two degrees per minute. RuCu-BTC-2 and RuCu-BTC-3 precursors, which are very similar to Ru–Cu@C-1 precursors, were utilized in the production of RuCu-BTC-2 and RuCu-BTC-3 samples, respectively. The optimized Ru–Cu@C-2 catalyst has been demonstrated to be an excellent HER catalyst because of its ultralow overpotential (20 mV at 10 mA cm^{-2}), ultralow Tafel slope (37 mV dec^{-1}), minor charge-transfer resistance (16.8), broad electrochemical active surface area, and superb stability. All these characteristics contribute to the catalyst's exceptional performance.[177]

4.8. AB & Cu-MOF composite

In a solution that included 2.5 mL of dimethylformamide, 2.5 mL of water, and 2.5 mL of ethanol, 20 mg of $Cu(OAc)_2$ and 21 mg of 1,3,5-benzenetricarboxylic acid were dissolved. Different results were obtained by altering the proportion of AB that was added to the mixtures (0.4, 0.7, and 1.7 wt%, respectively, based on Cu-BTC). After being sonicated, the substance was put into an autoclave made of stainless steel and lined with Teflon. It was then heated to 100 °C for twenty-four hours. The bluish-gray crystals that were collected were filtered, cleaned, dried, and weighed after being processed in a vacuum oven. The overpotential of the 1.7% AB/Cu-BTC composite is 208 mV when measured at a current density of 10 mA cm^{-2}, and the Tafel slope is 80 mV dec^{-1}. Table 3 shows the electrochemical activity of some reported hybrids.[178]

5. Critical aspects and future outlook

In the electrocatalytic and photocatalytic processes for the creation of hydrogen gas from water, materials based on copper have shown promising results. However, research on water splitting using copper-based materials as mediators is still in its early stages, and significant progress is still needed before systems using copper-based mediators can be considered competitive. For instance, this is a serious problem because catalysts based on copper (Cu), which has a stronger attraction for water molecules than carboxylate ligands, are not very resistant to water. This is because water molecules are more attracted to copper ions than carboxylate ligands. Grinding to an extremely fine powder is essential for recycling the great majority of copper-based products. In recent years, materials based on copper have made significant strides toward their goal of becoming highly active electrocatalysts for both the HER and the OER. Research on the electrochemical behaviour of copper-based materials in electrochemical water splitting is still in its infancy due to the breadth and complexity of the area. Therefore, the research is still in its infancy. Copper-based materials show promise as electrocatalysts for the HER and OER. These electrocatalysts can speed up kinetic processes and have found broad application in fields such as water-splitting systems and metal-air batteries. It is to be anticipated that further research will be carried out in this field. In addition, it is anticipated that an increase will occur in the utilization of materials based on copper in high-performance HER and OER.

In the future, it will be feasible to perform ground-breaking research on Cu-based catalysts thanks to modifications such as increasing the size of the metal active sites, doping them with additional active elements, employing conducting supports, and extending their size over conducting 3D supports. When working with sulfides, the ability to create vacancies in Cu-based structures without damaging the structure itself is also highly useful. It is possible to improve the efficiency of catalysts that are based on selenides by modifying the stoichiometry, making changes to the synthesis, or including additional active components. It has been proven that phosphates are excellent catalysts with activity levels comparable to those of catalysts based on transition metals. This analysis of catalysts based on copper provides a complete grasp of copper's potential as a powerful tool for enabling water splitting with high activity and stability. Copper's potential as a formidable instrument is

supplied by the review. In compounds such as oxides, hydroxides, LDHs, sulfides, selenides, and phosphides, it can also be used as a substitute for noble metals. Doping copper-based nanostructures with other metals, growing them *in situ* on three-dimensional metal foams, and utilizing conducting supports are some potential future tactics that might be used to increase the electrocatalytic activity of the nanostructures. Copper-based catalysts have the potential to one day serve as viable alternatives to noble elements for the creation of hydrogen through the electrocatalytic splitting of water, provided that additional structural changes are carried out to raise the surface-active sites.

6. Conclusions

The utilisation of effective alternative clean energy sources, energy conversion, and storage devices can help to reduce the depletion of oil and fossil fuel reserves. Both the OER and the HER are required to produce hydrogen from renewable resources, which is an essential step in the conversion of renewable energy into chemical energy that can be stored. As a result, it makes a lot of sense to develop catalysts that can accelerate the reaction rate by permitting multiple electron and proton coupling at low overpotentials. Because of its inexpensive price, ample supply, peculiar coordination chemistry, and varied redox characteristics, copper (Cu) is one of the most desirable transition metals. Cu-based nanoparticles employed as electrocatalysts can demonstrate a wide range of catalytic effects depending on their structure and composition. Although include all cases may be difficult, the purpose of this review is to provide an overview of the synthesis methods, distinct and vivid morphology, beneficial electrochemical properties, and performances of diverse Cu-based materials as electrocatalysts with exceptional OER and HER activity. In materials based on Cu in any of its valence states (Cu(0), Cu(I), Cu(II), *etc.* electrocatalytic activity for OER and HER is outstanding, exceedingly stable, and long-lasting. Due to their low electrical conductivity, Cu-based materials, which are new and have qualities such as abundance, efficiency, environmental friendliness, and low cost, are not suitable for water splitting catalysis. Even though most Cu-based compounds are still too weak due to poor activity and instability, progress has been made. As a result, researchers are continuously looking for new ways to improve.

According to the findings, the OER and HER activity of copper-based oxides and hydroxides is significantly lower than that of the other materials that were investigated. The apparent variation in activity can be reduced by raising the current density; nevertheless, this does not eliminate the problem entirely. Despite extended contact with the outside world, it is possible to achieve a high level of stability through the growth of conducting supports. Because they create metastable Cu ions, oxides based on copper, such as CuO and $Cu(OH)_2$, have significant OER activity. This is the case even when the metal itself is metastable. Due to the low electrical conductivity of the Cu-based oxides, the HER activity of these oxides was significantly lower when compared to that of other materials. When compared to oxide-based catalysts, the OER and HER activity levels of sulfide-based catalysts are significantly higher. The oxide or hydroxide phase that is generated during OER is the true catalyst, whereas the sulphides that are produced are only pre-catalysts. However, sulfide ions at the interface between the oxide and hydroxide might increase activity. In addition, copper sulphides were utilized for both OER and HER applications, and these sulphides were fortified with highly active and long-lasting sulphides that were derived from transition metals.

Data availability

No data was used for the research described in the article.

Conflicts of interest

The authors declare that they have no known competing financial interests or personal relationships that could have appeared to influence the work reported in this paper.

Acknowledgements

The Higher Education Commission of Pakistan supported this work under the grant designated as 2017/HEC/NRPU-10482.

References

1 Y. Liu, *et al.*, Metal sulfide/MOF-based composites as visible-light-driven photocatalysts for enhanced hydrogen production from water splitting, *Coord. Chem. Rev.*, 2020, **409**, 213220, DOI: 10.1016/j.ccr.2020.213220.

2 M. A. Rasool, *et al.*, An Insight into Carbon Nanomaterial-Based Photocatalytic Water Splitting for Green Hydrogen Production, *Catalysts*, 2023, **13**(1), DOI: 10.3390/catal13010066.

3 M. Ali, E. Pervaiz, T. Noor, O. Rabi, R. Zahra and M. Yang, Recent advancements in MOF-based catalysts for applications in electrochemical and photoelectrochemical water splitting: A review, *Int. J. Energy Res.*, 2021, **45**(2), 1190–1226, DOI: 10.1002/er.5807.

4 J. Joy, J. Mathew and S. C. George, Nanomaterials for photoelectrochemical water splitting – review, *Int. J. Hydrogen Energy*, 2018, **43**(10), 4804–4817, DOI: 10.1016/j.ijhydene.2018.01.099.

5 M. Mehrpooya and R. Habibi, A review on hydrogen production thermochemical water-splitting cycles, *J. Cleaner Prod.*, 2020, **275**, 123836, DOI: 10.1016/j.jclepro.2020.123836.

6 U. Sohail, E. Pervaiz, M. Ali, R. Khosa, A. Shakoor and U. Abdullah, Role of tungsten carbide (WC) and its hybrids in electrochemical water splitting application-A comprehensive review, *FlatChem*, 2022, 100404.

7 R. Khosa, E. Pervaiz, U. Abdullah, M. Ali, U. Sohail and A. Shakoor, An Insight on Molybdenum Phosphide and its Hybrids as Catalyst for Electrochemical Water splitting: A Mini-Review, *Mol. Catal.*, 2022, **528**, 112514.

8 N. Fajrina and M. Tahir, A critical review in strategies to improve photocatalytic water splitting towards hydrogen

production, *Int. J. Hydrogen Energy*, 2019, **44**(2), 540–577, DOI: 10.1016/j.ijhydene.2018.10.200.
9 W. Chen, *et al.*, A review on the visible light active modified photocatalysts for water splitting for hydrogen production, *Int. J. Energy Res.*, 2022, **46**(5), 5467–5477.
10 G. Kumar, *et al.*, Biomass based hydrogen production by dark fermentation—recent trends and opportunities for greener processes, *Curr. Opin. Biotechnol.*, 2018, **50**, 136–145, DOI: 10.1016/j.copbio.2017.12.024.
11 Z. Y. Hitit, C. Zampol Lazaro and P. C. Hallenbeck, Increased hydrogen yield and COD removal from starch/glucose based medium by sequential dark and photo-fermentation using clostridium butyricum and rhodopseudomonas palustris, *Int. J. Hydrogen Energy*, 2017, **42**(30), 18832–18843, DOI: 10.1016/j.ijhydene.2017.05.161.
12 D. Saadetnejad and R. Yıldırım, Photocatalytic hydrogen production by water splitting over Au/Al-$SrTiO_3$, *Int. J. Hydrogen Energy*, 2018, **43**(2), 1116–1122, DOI: 10.1016/j.ijhydene.2017.10.154.
13 E. B. Agyekum, C. Nutakor, A. M. Agwa and S. Kamel, A critical review of renewable hydrogen production methods: factors affecting their scale-up and its role in future energy generation, *Membranes*, 2022, **12**(2), 173.
14 S. Singla, S. Sharma, S. Basu, N. P. Shetti and T. M. Aminabhavi, Photocatalytic water splitting hydrogen production via environmental benign carbon based nanomaterials, *Int. J. Hydrogen Energy*, 2021, **46**(68), 33696–33717, DOI: 10.1016/j.ijhydene.2021.07.187.
15 M. Amin, *et al.*, Hydrogen production through renewable and non-renewable energy processes and their impact on climate change, *Int. J. Hydrogen Energy*, 2022, **47**, 33112–33134.
16 H. Ishaq, I. Dincer and C. Crawford, A review on hydrogen production and utilization: challenges and opportunities, *Int. J. Hydrogen Energy*, 2022, **47**(62), 26238–26264.
17 R. Solanki, *et al.*, Investigation of recent progress in metal-based materials as catalysts toward electrochemical water splitting, *J. Environ. Chem. Eng.*, 2022, **10**(4), 108207, DOI: 10.1016/j.jece.2022.108207.
18 F. Safari and I. Dincer, A review and comparative evaluation of thermochemical water splitting cycles for hydrogen production, *Energy Convers. Manage.*, 2020, **205**, 112182.
19 X. Chen and W. Shangguan, Hydrogen production from water splitting on CdS-based photocatalysts using solar light, *Front. Energy*, 2013, **7**(1), 111–118, DOI: 10.1007/s11708-012-0228-4.
20 J. Zhang, Q. Zhang and X. Feng, Support and Interface Effects in Water-Splitting Electrocatalysts, *Adv. Mater.*, 2019, **31**(31), 1808167, DOI: 10.1002/adma.201808167.
21 B. You and Y. Sun, Innovative Strategies for Electrocatalytic Water Splitting, *Acc. Chem. Res.*, 2018, **51**(7), 1571–1580, DOI: 10.1021/acs.accounts.8b00002.
22 A. Wu, *et al.*, Integrating the active OER and HER components as the heterostructures for the efficient overall water splitting, *Nano Energy*, 2018, **44**, 353–363, DOI: 10.1016/j.nanoen.2017.11.045.
23 W. Fang, *et al.*, Metal-organic framework derived Fe-Co-CN/reduced graphene oxide for efficient HER and OER, *Electrochim. Acta*, 2021, **365**, 137384, DOI: 10.1016/j.electacta.2020.137384.
24 J. E. Lee, *et al.*, Mini review on H_2 production from electrochemical water splitting according to special nanostructured morphology of electrocatalysts, *Fuel*, 2022, **308**, 122048.
25 B. T. Jebaslinhepzybai, T. Partheeban, D. S. Gavali, R. Thapa and M. Sasidharan, One-pot solvothermal synthesis of Co_2P nanoparticles: An efficient HER and OER electrocatalysts, *Int. J. Hydrogen Energy*, 2021, **46**(42), 21924–21938, DOI: 10.1016/j.ijhydene.2021.04.022.
26 S. Tan, W. Ouyang, Y. Ji and Q. Hong, Carbon wrapped bimetallic NiCo nanospheres toward excellent HER and OER performance, *J. Alloys Compd.*, 2021, **889**, 161528, DOI: 10.1016/j.jallcom.2021.161528.
27 R. Kripal, S. Ram, T. Lal Chandra and M. Upendra, Theoretical Zero Field Splitting Parameters of Fe^{3+} doped $TlGaSe_2$ Single Crystal, *Int. J. Appl. Eng. Res.*, 2021, **16**(4), 288–292.
28 S. Roy, *et al.*, Mechanistic insights into the promotional effect of Ni substitution in non-noble metal carbides for highly enhanced water splitting, *Appl. Catal., B*, 2021, **298**, 120560, DOI: 10.1016/j.apcatb.2021.120560.
29 H. Xu, H. Shang, C. Wang and Y. Du, Surface and interface engineering of noble-metal-free electrocatalysts for efficient overall water splitting, *Coord. Chem. Rev.*, 2020, **418**, 213374, DOI: 10.1016/j.ccr.2020.213374.
30 A. Q. Mugheri, A. A. Otho, M. A. Abro, A. Ali and S. Khan, Versatile noble-metal-free electrocatalyst synergistically accelerating for the highly comprehensive understanding evidence for Electrochemical Water Splitting: Future Achievements & Perspectives, *Surf. Interfaces*, 2021, **24**, 101104, DOI: 10.1016/j.surfin.2021.101104.
31 Q. Yang, *et al.*, Nanostructured heterogeneous photocatalysts for hydrogen production and water splitting: A comprehensive insight, *Appl. Mater. Today*, 2019, **17**, 159–182, DOI: 10.1016/j.apmt.2019.07.016.
32 I. Amorim and L. Liu, Transition metal tellurides as emerging catalysts for electrochemical water splitting, *Curr. Opin. Electrochem.*, 2022, 101031.
33 P. Meenapriya, Analysis of splitting of dust particles in the atmosphere using mathematical modeling Techniques, *Int. J. Sci. Res. Math. Stat. Sci.*, 2019, **6**(3), 1–11.
34 D. Li, H. Liu and L. Feng, A Review on Advanced FeNi-Based Catalysts for Water Splitting Reaction, *Energy Fuels*, 2020, **34**(11), 13491–13522, DOI: 10.1021/acs.energyfuels.0c03084.
35 T. Huang, *et al.*, Preparation of Al-Ga-In-Sn-Bi quinary alloy and its hydrogen production via water splitting, *Int. J. Hydrogen Energy*, 2015, **40**(5), 2354–2362, DOI: 10.1016/j.ijhydene.2014.12.034.
36 Z. Kou, *et al.*, Rational Design of Holey 2D Nonlayered Transition Metal Carbide/Nitride Heterostructure Nanosheets for Highly Efficient Water Oxidation, *Adv.*

Energy Mater., 2019, **9**(16), 1803768, DOI: 10.1002/aenm.201803768.

37 M. Hassan, M. M. Baig, K. H. Shah, A. Hussain, S. A. Hassan and A. Ali, MOF-based bimetallic diselenide nanospheres as a bifunctional efficient electrocatalysts for overall water splitting, *J. Phys. Chem. Solids*, 2022, **167**, 110780, DOI: 10.1016/j.jpcs.2022.110780.

38 W.-C. Oh, K. Ullah, L. Zhu, Z.-D. Meng, S. Ye and S. Sarkar, Photocatalytic properties under visible light with graphene based platinium selenide nanocomposites synthesized by microwave assisted method, *Mater. Sci. Semicond. Process.*, 2014, **25**, 34–42, DOI: 10.1016/j.mssp.2013.10.013.

39 B. Zhang, *et al.*, Designing MOF Nanoarchitectures for Electrochemical Water Splitting, *Adv. Mater.*, 2021, **33**(17), 2006042, DOI: 10.1002/adma.202006042.

40 D. Senthil Raja, X.-F. Chuah and S.-Y. Lu, In Situ Grown Bimetallic MOF-Based Composite as Highly Efficient Bifunctional Electrocatalyst for Overall Water Splitting with Ultrastability at High Current Densities, *Adv. Energy Mater.*, 2018, **8**(23), 1801065, DOI: 10.1002/aenm.201801065.

41 T. Ishaq, *et al.*, A perspective on possible amendments in semiconductors for enhanced photocatalytic hydrogen generation by water splitting, *Int. J. Hydrogen Energy*, 2021, **46**(79), 39036–39057, DOI: 10.1016/j.ijhydene.2021.09.165.

42 W. Wang, X. Xu, W. Zhou and Z. Shao, Recent Progress in Metal-Organic Frameworks for Applications in Electrocatalytic and Photocatalytic Water Splitting, *Adv. Sci.*, 2017, **4**(4), 1600371, DOI: 10.1002/advs.201600371.

43 Y. Fang, Y. Ma, M. Zheng, P. Yang, A. M. Asiri and X. Wang, Metal–organic frameworks for solar energy conversion by photoredox catalysis, *Coord. Chem. Rev.*, 2018, **373**, 83–115, DOI: 10.1016/j.ccr.2017.09.013.

44 M. Ni, M. K. H. Leung, D. Y. C. Leung and K. Sumathy, A review and recent developments in photocatalytic water-splitting using TiO2 for hydrogen production, *Renewable Sustainable Energy Rev.*, 2007, **11**(3), 401–425, DOI: 10.1016/j.rser.2005.01.009.

45 Y. Zhang, S. Yuan, G. Day, X. Wang, X. Yang and H.-C. Zhou, Luminescent sensors based on metal-organic frameworks, *Coord. Chem. Rev.*, 2018, **354**, 28–45, DOI: 10.1016/j.ccr.2017.06.007.

46 H. Li, K. Wang, Y. Sun, C. T. Lollar, J. Li and H.-C. Zhou, Recent advances in gas storage and separation using metal–organic frameworks, *Mater. Today*, 2018, **21**(2), 108–121, DOI: 10.1016/j.mattod.2017.07.006.

47 H. M. El-Bery and H. N. Abdelhamid, Photocatalytic hydrogen generation via water splitting using ZIF-67 derived Co3O4@C/TiO2, *J. Environ. Chem. Eng.*, 2021, **9**(4), 105702, DOI: 10.1016/j.jece.2021.105702.

48 A. R. Abbasi, M. Karimi and K. Daasbjerg, Efficient removal of crystal violet and methylene blue from wastewater by ultrasound nanoparticles Cu-MOF in comparison with mechanosynthesis method, *Ultrason. Sonochem.*, 2017, **37**, 182–191, DOI: 10.1016/j.ultsonch.2017.01.007.

49 B. Wei, J. Wu, G. Mei, Z. Qi, W. Hu and Z. Wang, NiCo2O4 nanowire arrays rich in oxygen deficiencies for hydrogen evolution reaction, *Int. J. Hydrogen Energy*, 2019, **44**(13), 6612–6617, DOI: 10.1016/j.ijhydene.2019.01.183.

50 A. Roy, D. Hursán, K. Artyushkova, P. Atanassov, C. Janáky and A. Serov, Nanostructured metal-N-C electrocatalysts for CO2 reduction and hydrogen evolution reactions, *Appl. Catal., B*, 2018, **232**, 512–520, DOI: 10.1016/j.apcatb.2018.03.093.

51 J. Song, X. Gu, J. Cheng, N. Fan, H. Zhang and H. Su, Remarkably boosting catalytic H_2 evolution from ammonia borane through the visible-light-driven synergistic electron effect of non-plasmonic noble-metal-free nanoparticles and photoactive metal–organic frameworks, *Appl. Catal., B*, 2018, **225**, 424–432, DOI: 10.1016/j.apcatb.2017.12.024.

52 R. Nivetha, *et al.*, Cu based Metal Organic Framework (Cu-MOF) for electrocatalytic hydrogen evolution reaction, *Mater. Res. Express*, 2020, **7**(11), 114001, DOI: 10.1088/2053-1591/abb056.

53 J.-B. Raoof, S. R. Hosseini, R. Ojani and S. Mandegarzad, MOF-derived Cu/nanoporous carbon composite and its application for electro-catalysis of hydrogen evolution reaction, *Energy*, 2015, **90**, 1075–1081, DOI: 10.1016/j.energy.2015.08.013.

54 W. Hong, *et al.*, Self-supported nanoporous cobalt phosphosulfate electrodes for efficient hydrogen evolution reaction, *Appl. Catal., B*, 2019, **251**, 213–219, DOI: 10.1016/j.apcatb.2019.03.070.

55 T. Song, *et al.*, Stable and improved visible-light photocatalytic hydrogen evolution using copper(II)–organic frameworks: engineering the crystal structures, *J. Mater. Chem. A*, 2017, **5**(13), 6013–6018, DOI: 10.1039/C7TA00095B.

56 R. Gupta, J. Shah, R. Singh and R. K. Kotnala, Nonphotocatalytic Water Splitting Process to Generate Green Electricity in Alkali Doped Zinc Oxide Based Hydroelectric Cell, *Energy Fuels*, 2021, **35**(11), 9714–9726, DOI: 10.1021/acs.energyfuels.1c01164.

57 H. L. Nguyen, Metal–organic frameworks for photocatalytic water splitting, *Sol. RRL*, 2021, **5**(7), 2100198.

58 S. Liu, Y.-J. Lei, Z.-J. Xin, Y.-B. Lu and H.-Y. Wang, Water splitting based on homogeneous copper molecular catalysts, *J. Photochem. Photobiol., A*, 2018, **355**, 141–151, DOI: 10.1016/j.jphotochem.2017.09.060.

59 I. Ullah, A. Munir, A. Haider, N. Ullah and I. Hussain, Supported polyoxometalates as emerging nanohybrid materials for photochemical and photoelectrochemical water splitting, *Nanophotonics*, 2021, **10**(6), 1595–1620, DOI: 10.1515/nanoph-2020-0542.

60 H. Tong, S. Ouyang, Y. Bi, N. Umezawa, M. Oshikiri and J. Ye, Nano-photocatalytic Materials: Possibilities and Challenges, *Adv. Mater.*, 2012, **24**(2), 229–251, DOI: 10.1002/adma.201102752.

61 P. Jiménez-Calvo, V. Caps and V. Keller, Plasmonic Au-based junctions onto TiO_2, gC_3N_4, and TiO_2-gC_3N_4 systems for photocatalytic hydrogen production:

Fundamentals and challenges, *Renewable Sustainable Energy Rev.*, 2021, **149**, 111095.
62 X. Chen, S. Shen, L. Guo and S. S. Mao, Semiconductor-based Photocatalytic Hydrogen Generation, *Chem. Rev.*, 2010, **110**(11), 6503–6570, DOI: **10.1021/cr1001645**.
63 M. Javed, *et al.*, Synthesis, characterization and photocatalytic applications of s-doped graphitic carbon nitride nanocomposites with nickel doped zinc oxide nanoparticles, *Dig. J. Nanomater. Biostructures*, 2020, **15**(4), 1097–1105.
64 A. A. Ismail and D. W. Bahnemann, Photochemical splitting of water for hydrogen production by photocatalysis: a review, *Sol. Energy Mater. Sol. Cells*, 2014, **128**, 85–101, DOI: **10.1016/j.solmat.2014.04.037**.
65 S. Z. Islam, A. Reed, N. Wanninayake, D. Y. Kim and S. E. Rankin, Remarkable Enhancement of Photocatalytic Water Oxidation in N_2/Ar Plasma Treated, Mesoporous TiO_2 Films, *J. Phys. Chem. C*, 2016, **120**(26), 14069–14081, DOI: **10.1021/acs.jpcc.6b02622**.
66 B. H. Nguyen and V. H. Nguyen, Recent advances in research on plasmonic enhancement of photocatalysis, *Adv. Nat. Sci.: Nanosci. Nanotechnol.*, 2015, **6**(4), 43001, DOI: **10.1088/2043-6262/6/4/043001**.
67 R. Shwetharani, M. Sakar, H. R. Chandan and R. Geetha Balakrishna, Observation of simultaneous photocatalytic degradation and hydrogen evolution on the lanthanum modified TiO_2 nanostructures, *Mater. Lett.*, 2018, **218**, 262–265, DOI: **10.1016/j.matlet.2018.02.031**.
68 J. C. Moore, R. Louder and C. V. Thompson, Photocatalytic Activity and Stability of Porous Polycrystalline ZnO Thin-Films Grown via a Two-Step Thermal Oxidation Process, *Coatings*, 2014, **4**(3), 651–699, DOI: **10.3390/coatings4030651**.
69 A. Kudo and Y. Miseki, Heterogeneous photocatalyst materials for water splitting, *Chem. Soc. Rev.*, 2009, **38**(1), 253–278.
70 R. M. Navarro Yerga, M. C. Alvarez Galvan, F. Del Valle, J. A. Villoria de la Mano and J. L. G. Fierro, Water splitting on semiconductor catalysts under visible-light irradiation, *ChemSusChem*, 2009, **2**(6), 471–485.
71 Y. Xu, M. Kraft and R. Xu, Metal-free carbonaceous electrocatalysts and photocatalysts for water splitting, *Chem. Soc. Rev.*, 2016, **45**(11), 3039–3052.
72 T. Jafari, *et al.*, Photocatalytic Water Splitting—the untamed dream: a review of recent advances, *Molecules*, 2016, **21**(7), 900, DOI: **10.3390/molecules21070900**.
73 Y. Liu, Y.-Y. Deng, Q. Zhang and H. Liu, Overview of recent developments of resource recovery from wastewater via electrochemistry-based technologies, *Sci. Total Environ.*, 2021, **757**, 143901.
74 L. Zhang, *et al.*, Recent advances in 1D electrospun nanocatalysts for electrochemical water splitting, *Small Struct.*, 2021, **2**(2), 2000048.
75 Y. Wang, B. Kong, D. Zhao, H. Wang and C. Selomulya, Strategies for developing transition metal phosphides as heterogeneous electrocatalysts for water splitting, *Nano Today*, 2017, **15**, 26–55, DOI: **10.1016/j.nantod.2017.06.006**.
76 B. You, M. T. Tang, C. Tsai, F. Abild-Pedersen, X. Zheng and H. Li, Enhancing Electrocatalytic Water Splitting by Strain Engineering, *Adv. Mater.*, 2019, **31**(17), 1807001, DOI: **10.1002/adma.201807001**.
77 B. You and Y. Sun, Hierarchically porous nickel sulfide multifunctional superstructures, *Adv. Energy Mater.*, 2016, **6**(7), 1502333.
78 H. Wang, *et al.*, Bifunctional non-noble metal oxide nanoparticle electrocatalysts through lithium-induced conversion for overall water splitting, *Nat. Commun.*, 2015, **6**(1), 1–8.
79 B. M. Hunter, H. B. Gray and A. M. Muller, Earth-abundant heterogeneous water oxidation catalysts, *Chem. Rev.*, 2016, **116**(22), 14120–14136.
80 B. You, *et al.*, Universal surface engineering of transition metals for superior electrocatalytic hydrogen evolution in neutral water, *J. Am. Chem. Soc.*, 2017, **139**(35), 12283–12290.
81 C. Chen, *et al.*, Highly crystalline multimetallic nanoframes with three-dimensional electrocatalytic surfaces, *Science*, 2014, **343**(6177), 1339–1343.
82 G. Liu, *et al.*, Promoting active species generation by plasmon-induced hot-electron excitation for efficient electrocatalytic oxygen evolution, *J. Am. Chem. Soc.*, 2016, **138**(29), 9128–9136.
83 Z. Chen, X. Duan, W. Wei, S. Wang and B.-J. Ni, Iridium-based nanomaterials for electrochemical water splitting, *Nano Energy*, 2020, **78**, 105270, DOI: **10.1016/j.nanoen.2020.105270**.
84 C. G. Morales-Guio, L.-A. Stern and X. Hu, Nanostructured hydrotreating catalysts for electrochemical hydrogen evolution, *Chem. Soc. Rev.*, 2014, **43**(18), 6555–6569.
85 Y. Guo, *et al.*, Nanoarchitectonics for transition-metal-sulfide-based electrocatalysts for water splitting, *Adv. Mater.*, 2019, **31**(17), 1807134.
86 Y. Yan, B. Y. Xia, B. Zhao and X. Wang, A review on noble-metal-free bifunctional heterogeneous catalysts for overall electrochemical water splitting, *J. Mater. Chem. A*, 2016, **4**(45), 17587–17603.
87 A. Lasia, Mechanism and kinetics of the hydrogen evolution reaction, *Int. J. Hydrogen Energy*, 2019, **44**(36), 19484–19518, DOI: **10.1016/j.ijhydene.2019.05.183**.
88 R. Paul, L. Zhu, H. Chen, J. Qu and L. Dai, Recent advances in carbon-based metal-free electrocatalysts, *Adv. Mater.*, 2019, **31**(31), 1806403.
89 C. Li and J.-B. Baek, Recent Advances in Noble Metal (Pt, Ru, and Ir)-Based Electrocatalysts for Efficient Hydrogen Evolution Reaction, *ACS Omega*, Jan. 2020, **5**(1), 31–40, DOI: **10.1021/acsomega.9b03550**.
90 J. Yan, *et al.*, Breaking Platinum Nanoparticles to Single-Atomic Pt-C_4 Co-catalysts for Enhanced Solar-to-Hydrogen Conversion, *Angew. Chem., Int. Ed.*, 2021, **60**(5), 2541–2547.
91 J. Theerthagiri, S. J. Lee, A. P. Murthy, J. Madhavan and M. Y. Choi, Fundamental aspects and recent advances in transition metal nitrides as electrocatalysts for hydrogen evolution reaction: a review, *Curr. Opin. Solid State Mater.*

Sci., 2020, **24**(1), 100805, DOI: 10.1016/j.cossms.2020.100805.
92 J. R. McKone, S. C. Marinescu, B. S. Brunschwig, J. R. Winkler and H. B. Gray, Earth-abundant hydrogen evolution electrocatalysts, *Chem. Sci.*, 2014, **5**(3), 865–878.
93 S. Bae, I. Jeon, J. Mahmood and J. Baek, Molybdenum-Based Carbon Hybrid Materials to Enhance the Hydrogen Evolution Reaction, *Chem. – Eur. J.*, 2018, **24**(69), 18158–18179.
94 W. Zhou, *et al.*, Recent developments of carbon-based electrocatalysts for hydrogen evolution reaction, *Nano Energy*, 2016, **28**, 29–43.
95 R. Wang, J. Han, X. Zhang and B. Song, Synergistic modulation in MX_2 (where M= Mo or W or V, and X= S or Se) for an enhanced hydrogen evolution reaction, *J. Mater. Chem. A*, 2018, **6**(44), 21847–21858.
96 X. Hou, Y. Li, L. Cheng, X. Feng, H. Zhang and S. Han, Cobalt-molybdenum disulfide supported on nitrogen-doped graphene towards an efficient hydrogen evolution reaction, *Int. J. Hydrogen Energy*, 2019, **44**(23), 11664–11674.
97 C. He, T. Bo, B. Wang and J. Tao, RGO induced one-dimensional bimetallic carbide nanorods: An efficient and pH-universal hydrogen evolution reaction electrocatalyst, *Nano Energy*, 2019, **62**, 85–93.
98 W. Li, B. Yu, Y. Hu, X. Wang, D. Yang and Y. Chen, Core–shell structure of $NiSe_2$ nanoparticles@ nitrogen-doped graphene for hydrogen evolution reaction in both acidic and alkaline media, *ACS Sustainable Chem. Eng.*, 2019, **7**(4), 4351–4359.
99 J. Ma, *et al.*, Polyaniline derived N-doped carbon-coated cobalt phosphide nanoparticles deposited on N-doped graphene as an efficient electrocatalyst for hydrogen evolution reaction, *Small*, 2018, **14**(2), 1702895.
100 W. Chen, *et al.*, Tungsten carbide–nitride on graphene nanoplatelets as a durable hydrogen evolution electrocatalyst, *ChemSusChem*, 2014, **7**(9), 2414–2418.
101 X. Liu, *et al.*, Metal (Ni, Co)-metal oxides/graphene nanocomposites as multifunctional electrocatalysts, *Adv. Funct. Mater.*, 2015, **25**(36), 5799–5808.
102 A. Ali and P. K. Shen, Nonprecious metal's graphene-supported electrocatalysts for hydrogen evolution reaction: fundamentals to applications, *Carbon Energy*, 2020, **2**(1), 99–121, DOI: 10.1002/cey2.26.
103 F. Safizadeh, E. Ghali and G. Houlachi, Electrocatalysis developments for hydrogen evolution reaction in alkaline solutions–a review, *Int. J. Hydrogen Energy*, 2015, **40**(1), 256–274.
104 R. Kirpal, pdf_paper_view @ isroset.org, 2022, [Online]. Available: https://isroset.org/pdf_paper_view.php?paper_id=2890&4-ISROSET-IJSRPAS-07965.pdf.
105 M. Ďurovič, J. Hnát and K. Bouzek, Electrocatalysts for the hydrogen evolution reaction in alkaline and neutral media. A comparative review, *J. Power Sources*, 2021, **493**, 229708, DOI: 10.1016/j.jpowsour.2021.229708.
106 Y.-J. Tang, *et al.*, Solid-phase hot-pressing of POMs-ZIFs precursor and derived phosphide for overall water splitting, *Appl. Catal., B*, 2019, **245**, 528–535.
107 J. Wang, *et al.*, Earth-abundant transition-metal-based bifunctional catalysts for overall electrochemical water splitting: a review, *J. Alloys Compd.*, 2020, **819**, 153346, DOI: 10.1016/j.jallcom.2019.153346.
108 H. Furukawa, K. E. Cordova, M. O'Keeffe and O. M. Yaghi, The chemistry and applications of metal–organic frameworks, *Science*, 2013, **341**(6149), 1230444.
109 C. R. Kim, T. Uemura and S. Kitagawa, Inorganic nanoparticles in porous coordination polymers, *Chem. Soc. Rev.*, 2016, **45**(14), 3828–3845.
110 Z. Wang and S. M. Cohen, Postsynthetic modification of metal–organic frameworks, *Chem. Soc. Rev.*, 2009, **38**(5), 1315–1329.
111 H. Furukawa, *et al.*, Ultrahigh porosity in metal-organic frameworks, *Science*, 2010, **329**(5990), 424–428.
112 Q. Wang and D. Astruc, State of the Art and Prospects in Metal–Organic Framework (MOF)-Based and MOF-Derived Nanocatalysis, *Chem. Rev.*, 2020, **120**(2), 1438–1511, DOI: 10.1021/acs.chemrev.9b00223.
113 P. Silva, S. M. F. Vilela, J. P. C. Tome and F. A. A. Paz, Multifunctional metal–organic frameworks: from academia to industrial applications, *Chem. Soc. Rev.*, 2015, **44**(19), 6774–6803.
114 J. Khan, N. Iqbal, A. Asghar and T. Noor, Novel amine functionalized metal organic framework synthesis for enhanced carbon dioxide capture, *Mater. Res. Express*, 2019, **6**(10), 105539.
115 L. E. Kreno, K. Leong, O. K. Farha, M. Allendorf, R. P. Van Duyne and J. T. Hupp, Metal–organic framework materials as chemical sensors, *Chem. Rev.*, 2012, **112**(2), 1105–1125.
116 N. Abdollahi, M. Y. Masoomi, A. Morsali, P. C. Junk and J. Wang, Sonochemical synthesis and structural characterization of a new Zn (II) nanoplate metal–organic framework with removal efficiency of Sudan red and Congo red, *Ultrason. Sonochem.*, 2018, **45**, 50–56.
117 M. S. Samuel, J. Bhattacharya, C. Parthiban, G. Viswanathan and N. D. P. Singh, Ultrasound-assisted synthesis of metal organic framework for the photocatalytic reduction of 4-nitrophenol under direct sunlight, *Ultrason. Sonochem.*, 2018, **49**, 215–221.
118 F. Zhang, T. Zhang, X. Zou, X. Liang, G. Zhu and F. Qu, Electrochemical synthesis of metal organic framework films with proton conductive property, *Solid State Ionics*, 2017, **301**, 125–132.
119 A. Carné-Sánchez, I. Imaz, M. Cano-Sarabia and D. Maspoch, A spray-drying strategy for synthesis of nanoscale metal–organic frameworks and their assembly into hollow superstructures, *Nat. Chem.*, 2013, **5**(3), 203–211.
120 P. A. Bayliss, *et al.*, Synthesis of metal–organic frameworks by continuous flow, *Green Chem.*, 2014, **16**(8), 3796–3802.
121 B. He, *et al.*, Continuous Flow Synthesis of a Zr Magnetic Framework Composite for Post-Combustion CO_2 Capture, *Chem. – Eur. J.*, 2019, **25**(57), 13184–13188.

122 J. Klinowski, F. A. A. Paz, P. Silva and J. Rocha, Microwave-assisted synthesis of metal–organic frameworks, *Dalton Trans.*, 2011, **40**(2), 321–330.
123 A. Huang, L. Wan and J. Caro, Microwave-assisted synthesis of well-shaped UiO-66-NH2 with high CO2 adsorption capacity, *Mater. Res. Bull.*, 2018, **98**, 308–313.
124 S. Rojas-Buzo, *et al.*, Tailoring Lewis/Brønsted acid properties of MOF nodes via hydrothermal and solvothermal synthesis: simple approach with exceptional catalytic implications, *Chem. Sci.*, 2021, **12**(29), 10106–10115.
125 Y. Liu, P. Ghimire and M. Jaroniec, Copper benzene-1, 3, 5-tricarboxylate (Cu-BTC) metal-organic framework (MOF) and porous carbon composites as efficient carbon dioxide adsorbents, *J. Colloid Interface Sci.*, 2019, **535**, 122–132.
126 R. Zhang, *et al.*, Tetrazole-based porous metal–organic frameworks for selective CO 2 adsorption and isomerization studies, *Dalton Trans.*, 2020, **49**(7), 2145–2150.
127 Y. Hao, Y. Xu, W. Liu and X. Sun, Co/CoP embedded in a hairy nitrogen-doped carbon polyhedron as an advanced tri-functional electrocatalyst, *Mater. Horiz.*, 2018, **5**(1), 108–115.
128 L. Qin, Z. Xu, Y. Zheng, C. Li, J. Mao and G. Zhang, Confined Transformation of Organometal-Encapsulated MOFs into Spinel $CoFe_2O_4$/C Nanocubes for Low-Temperature Catalytic Oxidation, *Adv. Funct. Mater.*, 2020, **30**(14), 1910257.
129 W. Zhou, *et al.*, Improved conductivity of a new Co (II)-MOF by assembled acetylene black for efficient hydrogen evolution reaction, *CrystEngComm*, 2018, **20**(33), 4804–4809.
130 K. Rui, *et al.*, Direct hybridization of noble metal nanostructures on 2D metal–organic framework nanosheets to catalyze hydrogen evolution, *Nano Lett.*, 2019, **19**(12), 8447–8453.
131 S. eun Kim and A. Muthurasu, Metal-organic framework–assisted bimetallic Ni@ Cu microsphere for enzyme-free electrochemical sensing of glucose, *J. Electroanal. Chem.*, 2020, **873**, 114356.
132 Y. H. Budnikova, Recent advances in metal–organic frameworks for electrocatalytic hydrogen evolution and overall water splitting reactions, *Dalton Trans.*, 2020, **49**(36), 12483–12502.
133 M. Nemiwal, V. Gosu, T. C. Zhang and D. Kumar, Metal organic frameworks as electrocatalysts: Hydrogen evolution reactions and overall water splitting, *Int. J. Hydrogen Energy*, 2021, **46**(17), 10216–10238, DOI: **10.1016/j.ijhydene.2020.12.146**.
134 W. Han, M. Li, Y. Ma and J. Yang, Cobalt-Based Metal-Organic Frameworks and Their Derivatives for Hydrogen Evolution Reaction, *Front. Chem.*, 2020, **8**, [Online]. Available: **https://www.frontiersin.org/articles/10.3389/fchem.2020.592915**.
135 Z. Fuqin, C. Zhang, G. Xiaohui, C. Du, Z. Zhuang and W. Chen, Immobilizing Pd nanoclusters into electronically conductive metal-organic frameworks as Bi-functional electrocatalysts for hydrogen evolution and oxygen reduction reactions, *Electrochim. Acta*, 2019, **306**, 627–634, DOI: **10.1016/j.electacta.2019.03.175**.
136 N. Planas, *et al.*, Defining the Proton Topology of the Zr6-Based Metal–Organic Framework NU-1000, *J. Phys. Chem. Lett.*, 2014, **5**(21), 3716–3723, DOI: **10.1021/jz501899j**.
137 X. Li, W. He, C. Li, B. Song and S. Liu, Synergetic surface modulation of ZnO/Pt@ ZIF-8 hybrid nanorods for enhanced photocatalytic CO_2 valorization, *Appl. Catal., B*, 2021, **287**, 119934.
138 F. Chen, S. Dong, Z. Wang, J. Xu, R. Xu and J. Wang, Preparation of mixed matrix composite membrane for hydrogen purification by incorporating ZIF-8 nanoparticles modified with tannic acid, *Int. J. Hydrogen Energy*, 2020, **45**(12), 7444–7454.
139 H. Yang, *et al.*, General synthetic strategy for libraries of supported multicomponent metal nanoparticles, *ACS Nano*, 2018, **12**(5), 4594–4604.
140 X. Dai, *et al.*, Molybdenum polysulfide anchored on porous Zr-metal organic framework to enhance the performance of hydrogen evolution reaction, *J. Phys. Chem. C*, 2016, **120**(23), 12539–12548.
141 F. Li, Q. Shao, X. Huang and J. Lang, Nanoscale trimetallic metal–organic frameworks enable efficient oxygen evolution electrocatalysis, *Angew. Chem.*, 2018, **130**(7), 1906–1910.
142 F. Li, *et al.*, Large-Scale, Bottom-Up Synthesis of Binary Metal–Organic Framework Nanosheets for Efficient Water Oxidation, *Angew. Chem.*, 2019, **131**(21), 7125–7130.
143 W. Cheng, H. Zhang, D. Luan and X. W. Lou, Exposing unsaturated Cu_1-O_2 sites in nanoscale Cu-MOF for efficient electrocatalytic hydrogen evolution, *Sci. Adv.*, 2021, **7**(18), eabg2580.
144 M. Wang, *et al.*, Site-Specified Two-Dimensional Heterojunction of Pt Nanoparticles/Metal–Organic Frameworks for Enhanced Hydrogen Evolution, *J. Am. Chem. Soc.*, 2021, **143**(40), 16512–16518.
145 Z. Xue, *et al.*, Missing-linker metal-organic frameworks for oxygen evolution reaction, *Nat. Commun.*, 2019, **10**(1), 1–8.
146 D. Liu, *et al.*, 3D porous Ru-doped NiCo-MOF hollow nanospheres for boosting oxygen evolution reaction electrocatalysis, *Inorg. Chem.*, 2021, **60**(8), 5882–5889.
147 X. Zhao, *et al.*, Mixed-node metal–organic frameworks as efficient electrocatalysts for oxygen evolution reaction, *ACS Energy Lett.*, 2018, **3**(10), 2520–2526.
148 D. S. Raja, H.-W. Lin and S.-Y. Lu, Synergistically well-mixed MOFs grown on nickel foam as highly efficient durable bifunctional electrocatalysts for overall water splitting at high current densities, *Nano Energy*, 2019, **57**, 1–13.
149 W. Cheng, S. Xi, Z.-P. Wu, D. Luan and X. W. Lou, In situ activation of Br-confined Ni-based metal-organic framework hollow prisms toward efficient electrochemical oxygen evolution, *Sci. Adv.*, 2021, **7**(46), eabk0919.
150 K. Kannimuthu, K. Sangeetha, S. S. Sankar, A. Karmakar, R. Madhu and S. Kundu, Investigation on nanostructured Cu-based electrocatalysts for improvising water splitting: a review, *Inorg. Chem. Front.*, 2021, **8**(1), 234–272.

151 P. Farinazzo Bergamo Dias Martins, P. Papa Lopes, E. A. Ticianelli, V. R. Stamenkovic, N. M. Markovic and D. Strmcnik, Hydrogen evolution reaction on copper: Promoting water dissociation by tuning the surface oxophilicity, *Electrochem. Commun.*, 2019, **100**, 30–33, DOI: 10.1016/j.elecom.2019.01.006.

152 L. Ye and Z. Wen, Self-supported three-dimensional Cu/Cu_2O–CuO/rGO nanowire array electrodes for an efficient hydrogen evolution reaction, *Chem. Commun.*, 2018, **54**(49), 6388–6391.

153 A. Tahira, Z. H. Ibupoto, M. Willander and O. Nur, Advanced Co_3O_4–CuO nano-composite based electrocatalyst for efficient hydrogen evolution reaction in alkaline media, *Int. J. Hydrogen Energy*, 2019, **44**(48), 26148–26157.

154 L. Yu, *et al.*, Hierarchical Cu@ CoFe layered double hydroxide core-shell nanoarchitectures as bifunctional electrocatalysts for efficient overall water splitting, *Nano Energy*, 2017, **41**, 327–336.

155 L. Yu, *et al.*, Cu nanowires shelled with NiFe layered double hydroxide nanosheets as bifunctional electrocatalysts for overall water splitting, *Energy Environ. Sci.*, 2017, **10**(8), 1820–1827.

156 Y.-S. Xie, Z. Wang, M. Ju, X. Long and S. Yang, Dispersing transition metal vacancies in layered double hydroxides by ionic reductive complexation extraction for efficient water oxidation, *Chem. Sci.*, 2019, **10**(36), 8354–8359.

157 Y. Zheng, *et al.*, Three-dimensional NiCu layered double hydroxide nanosheets array on carbon cloth for enhanced oxygen evolution, *Electrochim. Acta*, 2018, **282**, 735–742.

158 S. Hu, Y. Tan, C. Feng, H. Wu, J. Zhang and H. Mei, Synthesis of N doped NiZnCu-layered double hydroxides with reduced graphene oxide on nickel foam as versatile electrocatalysts for hydrogen production in hybrid-water electrolysis, *J. Power Sources*, 2020, **453**, 227872.

159 S. B. Kale, P. T. Babar, J.-H. Kim and C. D. Lokhande, Synthesis of one dimensional Cu 2 S nanorods using a self-grown sacrificial template for the electrocatalytic oxygen evolution reaction (OER), *New J. Chem.*, 2020, **44**(21), 8771–8777.

160 Y. Wang, Z. Ge, X. Li, J. Zhao, B. Ma and Y. Chen, Cu_2S nanorod arrays with coarse surfaces to enhance the electrochemically active surface area for water oxidation, *J. Colloid Interface Sci.*, 2020, **567**, 308–315.

161 L. He, *et al.*, Ultrarapid in situ synthesis of Cu_2S nanosheet arrays on copper foam with room-temperature-active iodine plasma for efficient and cost-effective oxygen evolution, *ACS Catal.*, 2018, **8**(5), 3859–3864.

162 L. An, *et al.*, Phase transformation fabrication of a Cu_2S nanoplate as an efficient catalyst for water oxidation with glycine, *Inorg. Chem.*, 2015, **54**(7), 3281–3289.

163 K. S. Bhat and H. S. Nagaraja, Hydrogen evolution reaction at extreme pH conditions of copper sulfide micro-hexagons, *J. Sci.: Adv. Mater. Devices*, 2020, **5**(3), 361–367.

164 X. Wang, *et al.*, Nitrogen-Doped Cu2S/MoS2 Heterojunction Nanorod Arrays on Copper Foam for Efficient Hydrogen Evolution Reaction, *ChemCatChem*, 2019, **11**(4), 1354–1361.

165 Q. Zhou, T.-T. Li, J. Wang, F. Guo and Y.-Q. Zheng, Hierarchical Cu2S NRs@ CoS core-shell structure and its derivative towards synergistic electrocatalytic water splitting, *Electrochim. Acta*, 2019, **296**, 1035–1041.

166 X. Wang, X. Hou, H. Lee, L. Lu, X. Wu and L. Sun, Copper Selenide–Derived Copper Oxide Nanoplates as a Durable and Efficient Electrocatalyst for Oxygen Evolution Reaction, *Energy Technol.*, 2020, **8**(7), 2000142.

167 W. Shi and J. Lian, Facile synthesis of copper selenide with fluffy intersected-nanosheets decorating nanotubes structure for efficient oxygen evolution reaction, *Int. J. Hydrogen Energy*, 2019, **44**(41), 22983–22990.

168 J. Masud, W. P. R. Liyanage, X. Cao, A. Saxena and M. Nath, Copper selenides as high-efficiency electrocatalysts for oxygen evolution reaction, *ACS Appl. Energy Mater.*, 2018, **1**(8), 4075–4083.

169 S. Anantharaj, *et al.*, Shrinking the hydrogen overpotential of Cu by 1 V and Imparting ultralow charge transfer resistance for enhanced H_2 evolution, *ACS Catal.*, 2018, **8**(7), 5686–5697.

170 J. Tian, Q. Liu, N. Cheng, A. M. Asiri and X. Sun, Self-supported Cu3P nanowire arrays as an integrated high-performance three-dimensional cathode for generating hydrogen from water, *Angew. Chem.*, 2014, **126**(36), 9731–9735.

171 S. Chu, *et al.*, Holey Ni-Cu phosphide nanosheets as a highly efficient and stable electrocatalyst for hydrogen evolution, *Appl. Catal., B*, 2019, **243**, 537–545.

172 A. Han, H. Zhang, R. Yuan, H. Ji and P. Du, Crystalline copper phosphide nanosheets as an efficient janus catalyst for overall water splitting, *ACS Appl. Mater. Interfaces*, 2017, **9**(3), 2240–2248.

173 S. Kumaravel, K. Karthick, P. Thiruvengetam, J. M. Johny, S. S. Sankar and S. Kundu, Tuning Cu Overvoltage for a Copper–Telluride System in Electrocatalytic Water Reduction and Feasible Feedstock Conversion: A New Approach, *Inorg. Chem.*, 2020, **59**(15), 11129–11141.

174 K. C. Majhi and M. Yadav, Transition metal chalcogenides based nanocomposites as efficient electrocatalyst for hydrogen evolution reaction over the entire pH range, *Int. J. Hydrogen Energy*, 2020, **45**(46), 24219–24231.

175 K. Yang, *et al.*, Ultrasmall Ru/Cu-doped RuO2 Complex Embedded in Amorphous Carbon Skeleton as Highly Active Bifunctional Electrocatalysts for Overall Water Splitting, *Small*, 2018, **14**(41), 1803009, DOI: 10.1002/smll.201803009.

176 X. Huang, Channel Rich RuCu Nanosheets for pH-Universal Overall Water Splitting Electrocatalysis, *Angew. Chem., Int. Ed.*, 2019, **58**, 14121–14126, DOI: 10.1002/anie.201908092.

177 M. Yang, *et al.*, Conversion of bimetallic MOF to Ru-doped Cu electrocatalysts for efficient hydrogen evolution in alkaline media, *Sci. Bull.*, 2020, **66**, 257–264, DOI: 10.1016/j.scib.2020.06.036.

178 X. Wang, *et al.*, Two facile routes to an AB&Cu-MOF composite with improved hydrogen evolution reaction, *J. Alloys Compd.*, 2018, **753**, 228–233, DOI: **10.1016/j.jallcom.2018.04.220**.

179 X. Liu, S. Cui, Z. Sun, Y. Ren, X. Zhang and P. Du, Self-supported copper oxide electrocatalyst for water oxidation at low overpotential and confirmation of its robustness by Cu K-edge X-ray absorption spectroscopy, *J. Phys. Chem. C*, 2016, **120**(2), 831–840.

180 S. M. Pawar, *et al.*, Self-assembled two-dimensional copper oxide nanosheet bundles as an efficient oxygen evolution reaction (OER) electrocatalyst for water splitting applications, *J. Mater. Chem. A*, 2017, **5**(25), 12747–12751.

181 F. Arshad, *et al.*, Controlled development of higher-dimensional nanostructured copper oxide thin films as binder free electrocatalysts for oxygen evolution reaction, *Int. J. Hydrogen Energy*, 2020, **45**(33), 16583–16590.

182 T. N. Huan, *et al.*, A dendritic nanostructured copper oxide electrocatalyst for the oxygen evolution reaction, *Angew. Chem., Int. Ed.*, 2017, **56**(17), 4792–4796.

183 B. Zhang, *et al.*, Nanostructured CuO/C hollow shell@ 3D copper dendrites as a highly efficient electrocatalyst for oxygen evolution reaction, *ACS Appl. Mater. Interfaces*, 2018, **10**(28), 23807–23812.

184 K. Karthick, *et al.*, Advanced Cu_3Sn and Selenized Cu_3Sn@Cu Foam as Electrocatalysts for Water Oxidation under Alkaline and Near-Neutral Conditions, *Inorg. Chem.*, 2019, **58**(14), 9490–9499, DOI: **10.1021/acs.inorgchem.9b01467**.

185 X. Ma, X. Li, A. D. Jagadale, X. Hao, A. Abudula and G. Guan, Fabrication of Cu $(OH)_2$@ NiFe-layered double hydroxide catalyst array for electrochemical water splitting, *Int. J. Hydrogen Energy*, 2016, **41**(33), 14553–14561.

186 S. B. Kale, P. T. Babar, J.-H. Kim and C. D. Lokhande, Synthesis of one dimensional Cu_2S nanorods using a self-grown sacrificial template for the electrocatalytic oxygen evolution reaction (OER), *New J. Chem.*, 2020, **44**(21), 8771–8777, DOI: **10.1039/D0NJ00909A**.

187 X. Xiong, C. You, Z. Liu, A. M. Asiri and X. Sun, Co-doped CuO nanoarray: an efficient oxygen evolution reaction electrocatalyst with enhanced activity, *ACS Sustainable Chem. Eng.*, 2018, **6**(3), 2883–2887.

188 J. Wang, L. Zhu, L. Ji and Z. Chen, Preparation of nanostructured Cu $(OH)_2$ and CuO electrocatalysts for water oxidation by electrophoresis deposition, *J. Mater. Res.*, 2018, **33**(5), 581–589.

189 L. Wang, *et al.*, Nickel enhanced the catalytic activities of amorphous copper for the oxygen evolution reaction, *J. Mater. Chem. A*, 2017, **5**(9), 4331–4334.

190 L. Ye and Z. Wen, Self-supported three-dimensional Cu/Cu_2O–CuO/rGO nanowire array electrodes for an efficient hydrogen evolution reaction, *Chem. Commun.*, 2018, **54**(49), 6388–6391, DOI: **10.1039/C8CC02510J**.